

Nanofluid flow and heat transfer in boundary layers: the influence of concentration diffusion  
on heat transfer enhancement

**Cintia Juliana Barbosa de Castilho**, Mark E. Fuller, Aakash Sane, Joseph T. C. Liu\*

School of Engineering EN2760 and Center for Fluid Mechanics,  
Brown University, Providence, Rhode Island 02912

\*Corresponding author: School of Engineering, Brown University, 184 Hope Street,  
Providence, RI 02912, USA. Tel 401-863-2654, fax 401-863-9028, joseph\_liu@brown.edu

The present work uses a perturbation procedure to deduce the small perturbation differential equations for velocity, temperature, and the diffusion equation for nanoparticle volume concentration. Thermalphysical variables are obtained from conventional means (e.g., mixture and field theory estimates) for nanofluids consisting of alumina nanoparticles dispersed in water (alumina-water nanofluid) and gold nanoparticles dispersed in water (gold-water nanofluid), and, in the case of gold-water nanofluid, molecular dynamics results are used to estimate such properties, including the transport coefficients. The very thin diffusion layer, at large Schmidt numbers, is found to have a great impact on the velocity and temperature profiles, owing to the transport property dependency and has a profound influence on surface conduction heat transfer rate enhancement and skin friction suppression for the case of nanofluid concentration withdrawal at the wall. In this case, the diffusional heat transfer rate is negligible, again, owing to the large Schmidt numbers encountered. Possible experiments directed at this interesting phenomenon are discussed.

## **INTRODUCTION**

“Nanofluids” is commonly understood as fluids containing well-dispersed and dilute particles of nanometer dimensions, usually metallic. Its designation was given in the pioneering work of Choi [1]. The attraction is that nanofluids have thermal conductivities superior to that of the base fluid and that, when used in micron-sized channels or tubes, could promote surface heat transfer rate enhancement and yet will be less likely to cause blockage. The applications of nanofluids were reviewed in the book by Das et al. [2] and by Das, et al. [3], and more recently, the properties of nanofluids by Paolucci and Puliti [4]. Very comprehensive measurements of nanofluid thermal conductivity by multiple laboratories were reported by Buongiorno, et al. [5] and that of viscosity measurements by Venerus, et al. [6]. The thermal conductivity measurements did not show the spectacular enhancement as anticipated earlier, but more aligned with mean field theories of Maxwell [7] and Rayleigh [8] and their variants. Although at the time of Maxwell and Rayleigh when “nano” was not common, present researchers adopted their formalism of “small” obstructions embedded in fluids to nanofluids (e.g., [5]). Viscosity measurements of well-dispersed nanoparticles exhibited a Newtonian fluid behavior [6].

The question that naturally arises is that what are the convective effects, such as forced convection nanofluid flow in a boundary layer, which resembles the leading edge and entrance region of flow in channels and tubes as observed by Wen and Ding [9] and Jung et al. [10], among others. If we focus on surface heat transfer rate owing to thermal conduction alone, while nanofluid thermal conductivity enhances the surface heat transfer rate explicitly in the Fourier relation. Enhanced thermal conductivity also spreads out the temperature profile according to the thermal boundary layer equation and thus tends to decrease surface heat transfer rate. Forced convection effects, or inertia effects, have the tendency to steepen the temperature profile. These mechanisms are brought out in the small nanofluid volume

fraction perturbation theory for plug flow [11] and for the laminar boundary layer in the special case of zero volume fraction flux at a solid wall [12].

The general formulation [13] of convective heat transfer in a nanofluid brings in the possibility of diffusion flux transport of thermal energy owing to Brownian diffusion of nanoparticles in Einstein's sense [14]. It is the assessment of the relative magnitude of this additional heat transfer mechanism relative to conduction heat transfer in boundary layers [12] that is a central discussion in the present paper.

### ***LAMINAR BOUNDARY LAYER EQUATIONS FOR A NANOFLUID***

The continuum description of nanofluid flow and heat transfer is presented by Buongiorno [13]. The fundamental equations in boundary layer form are obtained by Pfautsch [15]. Based on a perturbation theory motivated by the experimental prevalence of small nanoparticle volume fraction, applications to the Rayleigh-Stokes flow, or plug flow, is given by Liu [11] and to boundary layers for uniform volume fraction by Liu et al. [12]. The latter is brought about by zero-nanofluid volume flux at a solid wall. Before studying the laminar boundary layer equations in detail for the active participation of nanofluid volume fraction diffusion, it would be helpful to obtain an estimate of the relative magnitude of thermal energy transfer by heat conduction and by diffusion.

It is already estimated that the effects of thermal diffusion is relatively weak compared to the possibility of mass diffusion by the Einstein mechanism [14] of bombardment of nanoparticles by the random motion of the base-fluid molecules [13]. Thus, it is sufficient to treat the diffusion process as one of binary diffusion for which the diffusion current, relative to a mass averaged velocity, is approximated by Fick's Law in terms of the nanofluid mass fraction. The Brownian diffusion coefficient is then identified with the binary diffusion coefficient. The mass fraction, in turn, is converted to the nanoparticle volume

fraction for dilute concentration. This then, is the thought process leading to the diffusion equation presented by Buongiorno [13], following the formalisms in texts and monographs on transport phenomena and physicochemical hydrodynamics [16,17]. A recent review of the continuum description of nanofluid is given by Nield and Kuznetsov [18], but the nanofluid properties discussed did not progress from the mixture theory.

The boundary layer form of the heat transfer rate is

$$q = -k \frac{\partial T}{\partial y} + j_p h_p = - \left[ k \frac{\partial T}{\partial y} + \rho D \frac{\partial X_p}{\partial y} h_p \right] \quad \text{eq. (1)}$$

where  $j_p$  is the nanoparticle phase diffusion current and is, in terms of the nanoparticle volume fraction  $\phi$ , equal to  $-\rho_p D \partial \phi / \partial y + \mathcal{O}(\phi^2)$  to order  $\mathcal{O}(\phi^2)$  for  $\phi \ll 1$ , after relating the mass fraction to volume fraction. The heat transfer rate, for nonuniform distribution of the nanoparticle concentration, now includes the diffusion current transport of nanoparticle thermal energy  $h_p$ . This is reminiscent of the discussion of heat transfer a reacting fluid [19].

In order to analyze the surface heat transfer rate, the boundary layer profiles from the conservation equations need to be solved, subject to boundary conditions. Aside from the inherent interest of boundary layers, they are also important to the study the entrance region of channels and tubes where the observed nanofluid heat transfer enhancement is much more “spectacular” than the downstream developed region. For simplicity, the two-dimensional system at constant pressure is studied, from which complex extensions could always be made.

Continuity equation

$$\frac{\partial \rho u}{\partial x} + \frac{\partial \rho v}{\partial y} = 0 \quad \text{eq. (2)}$$

Momentum equation

$$\rho \left( u \frac{\partial u}{\partial x} + v \frac{\partial v}{\partial y} \right) = \frac{\partial}{\partial y} \left( \mu \frac{\partial u}{\partial y} \right) \quad \text{eq. (3)}$$

Energy equation

$$\rho \left( u \frac{\partial h}{\partial x} + v \frac{\partial h}{\partial y} \right) = - \frac{\partial q}{\partial y} = \frac{\partial}{\partial y} \left( k \frac{\partial T}{\partial y} + \rho_p D \frac{\partial \phi}{\partial y} h_p \right) \quad \text{eq. (4)}$$

Volume fraction diffusion equation

$$\left( u \frac{\partial \phi}{\partial x} + v \frac{\partial \phi}{\partial y} \right) = \frac{\partial}{\partial y} \left( D \frac{\partial \phi}{\partial y} \right) \quad \text{eq. (5)}$$

The energy equation is written in “incompressible” form in the sense of Lagerstrom [20]: for low Mach numbers, the rate of viscous dissipation is neglected as well as the work done by the pressure gradient; the transport properties are functions only of the volume fraction and otherwise in their small temperature-loading form. The nanofluid static enthalpy is  $dh = c dT$ , where  $C$  is the nanofluid heat capacity and is a function of the volume fraction  $\phi$ . The nanoparticle phase static enthalpy is  $dh_p = c_p dT$ , where  $c_p$  is the nanoparticle heat capacity. The base fluid and nanoparticles are considered to be in thermal equilibrium [13] and thus they have the same absolute temperature  $T$ .

The other thermophysical properties such as nanofluid density and heat capacity, are functions of the nanofluid volume fraction. These “equations of state” are discussed in the next section.

The boundary conditions are

$$\begin{aligned} y=0: & \quad u=0, \quad T=T_w, \quad \phi=\phi_w \\ y=\infty: & \quad u=U, \quad T=T_\infty, \quad \phi=\phi_\infty \end{aligned} \quad \text{eq. (6)}$$

The boundary condition for the volume fraction corresponding to zero flux at a solid wall,

$y=0: \partial\phi/\partial y=0$ , yields the solution  $\phi=\phi_\infty$ . In this case, the heat transfer rate is through

thermal conduction alone, devoid participation of the diffusional current transport of thermal energy [12]. The condition  $y=0: \phi = \phi_w$  corresponds to the situation of a porous wall in which the levels of volume fraction at could be maintained. This situation, which give rise to nanoparticle diffusion current, will contribute to the diffusional transport of thermal energy as an additional contributing factor the heat transfer rate at the wall as well as giving rise to variations of volume fraction-dependent thermophysical properties.

### ***THERMOPHYSICAL PROPERTIES***

Enhanced thermal conductivity of nanofluids incited the initial enthusiastic studies of such fluids for cooling purposes [1-3]. Since then, benchmark measurements of nanofluid conductivities through efforts of a wide assembly of laboratories have been reported [5] as well as that for viscosity [6]. It appears that thermal conductivities are more aligned with field theories and that nanofluids behave very much like a Newtonian fluid. Thermophysical properties are expressible in terms of the volume fraction, particularly in terms of ascending powers of  $\phi$  with the slope at  $\phi = 0$  as coefficient of the first linear term. It is found that this is convenient in that the slope could be evaluated using mixture theory such as for density and heat capacity, or from molecular dynamics simulation results. Transport coefficients are measured and expressed as a similar representation in terms of  $\phi$  as are expressions from field theories and simulations. The dimensionless density and density-heat capacity are represented as

$$\rho^* = \rho / \rho_f + \phi_{\infty} (\rho^*)'_{\phi=0} \Phi + \mathcal{G}(\phi_{\infty}^2) \quad \text{eq. (7)}$$

$$\rho^* c^* = \rho c / \rho_f c_f + \phi_{\infty} (\rho^* c^*)'_{\phi=0} \Phi + \mathcal{G}(\phi_{\infty}^2) \quad \text{eq. (8)}$$

where the prime indicates differentiation with respect to the volume fraction is normalized by that in the free stream. The dynamic viscosity and thermal conductivity are similarly expressed as

$$\mu^* = \mu / \mu_f = 1 + \phi_\infty (\mu^*)'_{\phi=0} \Phi + \mathcal{O}(\phi_\infty^2) \quad \text{eq. (9)}$$

$$k^* = k / k_f = 1 + \phi_\infty (k^*)'_{\phi=0} \Phi + \mathcal{O}(\phi_\infty^2) \quad \text{eq. (10)}$$

where the dimensionless volume fraction distribution is defined as  $\Phi = \phi / \phi_\infty$ . The free stream volume fraction is low,  $\phi_\infty \ll 1$ , which is prevalent in experimental measurements and commensurate with dilute nanoparticle concentration for nanofluids. It is the natural expansion parameter in a simple perturbation theory [11].

The diffusion coefficient, which is identified with that for Brownian diffusion, is [13,14]

$$D = k_B T / 6\pi\mu_f r_d \quad \text{eq. (11)}$$

Recollecting that the reduction to “incompressible” form of the basic equations in fluid mechanics, Lagerstrom [20] discussed the double expansion in terms of the (low) Mach number and small relative temperature loading, which rendered the viscosity coefficient and thermal conductivity to be independent of the temperature. The Brownian diffusion coefficient, which is explicitly expressed as a linear function of the temperature, is taken as constant. The temperature in which the transport coefficients are evaluated would be an averaged temperature.

## ***PERTURBATION EXPANSION FOR $\phi_\infty \ll 1$***

The thermophysical properties are already in an ascending series in the perturbation parameter  $\phi_\infty$ , the dependent variables, symbolically represented by  $Q$ , are expanded accordingly as

$$Q^* = Q/Q_f = Q_0 + \phi_\infty Q_1 + \mathcal{O}(\phi_\infty^2) \quad \text{eq. (12)}$$

where the zeroth order is that of the base fluid, devoid of nanoparticles, the first order term is the nanofluid perturbation for small volume fraction. One can always perform the perturbation expansion on the physical conservation equations, and subsequently seek similar solutions for the first order perturbation. The zeroth order velocity is that of the Blasius function and the temperature that of Pohlhausen function for heat transfer discussed extensively in Schlichting [21].

After straightforward manipulations, the resulting zeroth and first order problems are recast into the Blasius similarity dependent variable

$$\eta = \frac{y}{\sqrt{\nu_f x/U}} = \frac{y^*}{\sqrt{x^*/\text{Re}}} \quad \text{eq. (13)}$$

and stream function

$$\psi^* = \frac{\psi}{UL} = \sqrt{\frac{x^*}{\text{Re}}} f(\eta) \quad \text{eq. (14)}$$

from which

$$u^* = f'(\eta), \quad v^* = (2\sqrt{x^*/\text{Re}})^{-1}(\eta f' - f) \quad \text{eq. (15)}$$

Prime indicates differential with respect to  $\eta$ . The perturbation expansion (12) carries over to the Blasius form of the stream function; the zeroth and first order problems are discussed in the following.

The perturbation expansion (12) and the implied expansions of the properties (6) and (8) and the similarity variable transform (13)-(15) applied to the continuity and momentum equations (2) and (3) result in the sequence of problems. The zeroth order velocity function is the Blasius function, it is stated as it is an input to the perturbation velocity function

$$\begin{aligned} f_0''' + 2^{-1} f_0 f_0'' &= 0 \\ f_0(0) = f_0'(0) &= 0, \quad f_0'(0) = 1 \end{aligned} \quad \text{eq. (16)}$$

The first order nanofluid velocity function is subjected to the volume fraction-dependent viscosity coefficient, which accounts for the presence of  $\Phi$  and  $\Phi'$  associated with  $(\mu^*)'_{\phi=0}$ , while the inertia effect of the nanofluid density, which is volume fraction-dependent, is reflected in  $(\rho^*)'_{\phi=0}$  associated with  $\Phi$  but has been moved from the inertia-left side to the right side

$$\begin{aligned} f_1''' + 2^{-1} (f_0 f_1'' + f_1 f_0'') &= 2^{-1} \left[ (\mu^*)'_{\phi=0} - (\rho^*)'_{\phi=0} \right] \Phi f_0 f_0'' + (\mu^*)'_{\phi=0} \Phi' f_0'' \\ f_1(0) = f_1'(0) &= 0, \quad f_1'(0) = 0 \end{aligned} \quad \text{eq. (17)}$$

The boundary conditions are already satisfied by the zeroth order problem, thus the inhomogeneous first order problem satisfy homogeneous boundary conditions. The volume fraction-dependent has its effect only when there is a volume fraction gradient, reflected by the presence of  $\Phi'(\eta)$  in the differential equation on (17). This explicit dependence is lost in the case when  $\Phi$  is uniform across the boundary layer as in the case of zero-nanoparticle flux at the wall [12] where  $\Phi(\eta) = 1$  in consideration of the diffusion equation (5) for the zero-flux boundary condition.

Similar expansion using (8) and (10) and defining the dimensionless temperature as  $\theta = (T - T_\infty)/(T_w - T_\infty)$ , and applying to the energy equation (4) result in a sequence of

problems as for the velocity problem. The zeroth order problem is just that of Pohlhausen's (see Schlichting [20]) heat transfer problem, where  $\theta$  is similarly expanded as in (12)

$$\begin{aligned}\theta_0'' + (\text{Pr}_f/2) f_0 \theta_0' &= 0 \\ \theta_0(0) &= 1, \quad \theta_0(\infty) = 0\end{aligned}\tag{eq. (18)}$$

The first order temperature problem is **eq. (19)**

As with the velocity profile, the boundary conditions are already satisfied by the zeroth order problem, thus the inhomogeneous first order problem satisfies homogeneous boundary conditions. The effect of the thermal conductivity's dependence on the volume fraction is reflected by terms associated with  $(k^*)'_{\phi=0}$ . That associated with the inertia effect of heat capacity, which originally is on the **left-hand** side, is associated with  $(\rho^* c^*)'_{\phi=0}$ . The mechanism of diffusion current in transporting thermal energy is reflected in the last term in (19) where the diffusion coefficient is buried in the base-fluid Schmidt number. This has an effect as long as the volume fraction, from the diffusion equation (5), is nonuniform across the boundary layer.

The volume fraction is already a first order perturbation as the zeroth problem is for the base fluid and absence of nanoparticles through the formalism of expansion (12). In similarity form, the normalized volume fraction satisfies

$$\begin{aligned}\Phi'' + (\text{Sc}_f/2) f_0 \Phi' &= 0 \\ \Phi(0) &= \Phi_w, \quad \Phi(\infty) = 1\end{aligned}\tag{eq. (20)}$$

### ***Solutions of the similarity problems***

The Blasius solution for (16) is well known [21] but it is numerically solved again because of its necessary input to all the first order nanofluid problems (17), (19), (20) which require numerical solution.

The zeroth order temperature problem (18) yields the Pohlhausen integral in terms of the Blasius function [20]

$$\theta_0(\eta; \text{Pr}_f) = \int_{\eta}^{\infty} [f''(\xi)]^{\text{Pr}_f} d\xi \bigg/ \int_0^{\infty} [f''(\xi)]^{\text{Pr}_f} d\xi \quad \text{eq. (21)}$$

It is actually more convenient to solve (18) numerically for input to the first order problem (19) than to use the numerical evaluation of the integrals in terms of the Blasius velocity functions. Nevertheless, the correlation of results of the latter gives a convenient formula for the heat transfer parameter [21]

$$-\theta'_0(0; \text{Pr}_f) \cong 0.332 \sqrt[3]{\text{Pr}_f} \quad \text{eq. (22)}$$

in the range  $0.6 < \text{Pr}_f < 10$ .

The volume fraction diffusion equation (20) for  $\Phi$  is similar to that for  $\theta_0$  except for the boundary conditions and presence of  $\text{Sc}_f$  in place of  $\text{Pr}_f$ . If we let  $\varphi = (\Phi - 1) / (\Phi_w - 1)$ , which is independent of the wall value  $\Phi_w$ , and which also satisfies a similar dimensionless differential equation with the same boundary conditions as  $\theta_0$ , but with  $\text{Sc}_f$  replacing  $\text{Pr}_f$ ,

$$\begin{aligned} \varphi'' + (\text{Sc}_f / 2) f_0 \varphi' &= 0 \\ \varphi(0) &= 1, \quad \varphi(\infty) = 0 \end{aligned} \quad \text{eq. (23)}$$

then

$$\varphi(\eta; \text{Sc}_f) = \int_{\eta}^{\infty} [f''(\xi)]^{\text{Sc}_f} d\xi \bigg/ \int_0^{\infty} [f''(\xi)]^{\text{Sc}_f} d\xi \quad \text{eq. (24)}$$

for which the wall parameter, inferred from [21], is

$$-\varphi'(0) \cong 0.339 \sqrt[3]{\text{Sc}_f} \quad \text{eq. (25)}$$

for  $\text{Sc}_f \gg 1$ . The dimensionless volume fraction  $\Phi$  is thus

$$\begin{aligned} \Phi(\eta; Sc_f) &= 1 + (\Phi_w - 1)\varphi(\eta; Sc_f) \\ -\Phi'(0; Sc_f) &\cong (\Phi_w - 1) 0.339 \sqrt[3]{Sc_f}, \quad Sc_f \gg 1 \end{aligned} \quad \text{eq. (26)}$$

It can be easily observed from the homogeneous volume fraction diffusion equation (19) that the condition of zero flux at the wall [12] is equivalent to the solution for the boundary condition  $\Phi_w = 1$ , which gives a constant volume fraction distribution  $\Phi(\eta; Sc_f) = 1$  throughout the boundary layer according to eq. (26).

## RESULTS FOR ALUMINA-WATER NANOFLUID

Properties for alumina are available from mixture calculations, where the respective

$$(\rho^*)'_{\phi=0, mix} = 2.89, \quad (\rho^*c^*)'_{\phi=0, mix} = -0.18$$

slopes are obtained by using mixture formulas . For dilute spherical nanoparticles, the nanofluid behaves like a Newtonian fluid and Einstein's

result  $(\mu^*)'_{\phi=0, mix} = 2.50$  is satisfactory [6, 13]. The classical result from Maxwell [5, 7, 13]

gives  $(k^*)'_{\phi=0, Maxwell} = 3.00$  . But Wen and Ding's [9] explicit measurements in water-based

aluminum oxide gave  $(k^*)'_{\phi=0, Wen\&Ding} = 6.00$  , which will be used here.

The zeroth order Blasius velocity profile  $f_0'(\eta)$  and the Pohlhausen temperature profile  $\theta_0(\eta)$  for the base fluid, in absence of nanoparticles, are shown in Figure 1 as

reference to compare with the perturbation profiles to follow. The influence of nanofluid volume fraction at the wall is reflected by the three values of the boundary condition chosen, .

$$\Phi(0) = 0, 1, 2$$

. The condition unity is the “insulated wall” case where there is zero nanoparticle flux at the wall (Figure 2).

$$\Phi(0) = 0$$

The condition implies a depletion of nanoparticle concentration at the wall,

for instance, through a porous matrix at the wall. The sharp gradient in  $\Phi(\eta)$  near the wall in

a very thin concentration layer for large  $Sc_f = 2 \times 10^4$ , causes reversals in both  $\theta_1(\eta)$  and

$$f_1'(\eta)$$

as shown in Figure 3a. The wall region is shown in Figure 3b. The ratio of the very

thin diffusion layer relative to the thermal layer is estimated by  $\delta_\phi / \delta_\theta \approx (Pr_f / Sc_f)^{1/2} \approx 0.02$ ,

as depicted in Figures 3a and 3b. The Schmidt number value is estimated by taking the average nanoparticle diameter to be approximately 10nm. The Schmidt number correspondingly decreases as the nanoparticle average diameter increases so that

$$Sc_f \approx 2 \times 10^3$$

for 100nm diameter; in any case, the diffusion layer remains relatively very thin

$$\delta_\phi / \delta_\theta \approx 0.06$$

and the qualitative effects are expected to be similar.

$$\Phi(0) = 2.0$$

For the case, which implies that there is added concentration of nanoparticles near the wall than that of the “insulated wall” case (Figure 2), the effect of the

diffusion layer is to steepen the  $\theta_1(\eta)$  and  $f_1'(\eta)$  profiles (Figure 4a) within the region of the thin diffusion layer in Figure 4b.

The wall region effect of the diffusion layer is summarized in Table 1 for the three-

boundary value of  $\Phi(0)$  of the first column.

We are reminded that  $\eta$  is a function of the Blasius solution and according to eq. (26) and eq. (24).

## **RESULTS FOR GOLD-WATER NANOFLUIDS**

There are two cases with respect to the manner in which thermophysical properties are estimated. One is using mixture theory to evaluate the density and heat capacity, which is known to be somewhat questionable in spite of their prevalent use. The other is to estimate properties from molecular dynamics results, including transport properties. The latter, which is more fundamental, has become available recently for, in particular, gold-water nanofluids in publications associated with Puliti [22, 23].

### **Mixture Results**

We return to the representation of properties as functions of the nanoparticle volume fraction as (7)-(10). Mixture results for the gold-water nanofluid density and density-heat capacity product in terms of the slopes at zero nanofluid volume fraction are

$$(\rho^*)'_{\phi=0,MIX} = 18.30 \quad (\rho^*c^*)'_{\phi=0,MIX} = -0.42$$

and . The viscosity coefficient slope is also taken to

$$(\mu^*)'_{\phi=0,mix} = 2.50.$$

be that from Einstein's value The Maxwell-Lord Rayleigh estimate of the

$$(k^*)'_{\phi=0,Maxwell} = 3$$

thermal conductivity is used, for which . These are summarized in [12].

$$\Phi(0) = 0$$

The case, which represent a depletion of nanoparticles (Figures 5a, 5b) is modified from the zero-flux solid wall case of Figure 6. The negative slope of the perturbation temperature profile in Figure 6 is rendered more negative in Figures 5a and 5b;

$$\Phi(0) = 2$$

for , Figures 7a and 7b, the perturbation temperature slope near the wall becomes positive. The slope of the perturbation velocity profile is already positive for the solid wall case (Figure 6), the depletion condition  $\Phi(0) = 0$  has the similar effect of decreasing the

$$\Phi(0) = 2$$

velocity slope near the wall, while the condition increases the perturbation velocity profile slope (Figure 7a and 7b). These effects are summarized in Table 2.

### ***Properties estimated from Molecular Dynamics***

It is generally regarded that the properties estimated from molecular dynamics computations [4, 21, 22] would be fundamental compared to that obtained by postulating a mixture for the nanofluid. It is fortunate that molecular dynamics thermophysical property

results are available for gold-water nanofluid so that their utilization in the continuum description of gold-water nanofluid flow and heat transfer can be compared to that using mixture property results for the “porous matrix wall” calculations at differing wall boundary conditions for the nanofluid volume fraction. Summarized in [12] are the estimates obtained from molecular dynamics **results [21, 22]**, referring to the representation depicted in (12):

$$(\rho^*)'_{\phi=0,MD} = 18.7, (\rho^*C^*)'_{\phi=0,MD} = -2.37.$$

Molecular dynamics simulation for viscosity and thermal conductivity of gold-water nanofluids appear only in the thesis of Puliti [21] and are subjected to interpretation in order to bring the results into practical usage form [12] which

$$(\mu^*)'_{\phi=0,MD} = 10, (k^*)'_{\phi=0,MD} = 20.$$

resulted in the values used in the present paper,

The solid wall, zero flux results **(Figure 8)** for which  $\Phi(\eta) = 1$  throughout the boundary layer, are qualitatively similar to the  $\Phi(0) = 0$  **(Figure 9a)** and  $\Phi(0) = 2$  **(Figure 10a)** only in the outer regions of the boundary layer. The inner regions of both first order temperature and velocity profiles subjected to the depletion boundary condition  $\Phi(0) = 0$  show reversals **Figures 9a and 9b** as influenced by the sharp volume concentration layer. In contrast, the inner region of the boundary layer subjected to the additional volume concentration  $\Phi(0) = 2$  through the thin concentration layer increases the steepness of both the first order velocity and temperature profiles (Figure 10a and 10b) in comparison with the

“insulated wall” case of Figure 8. A summary of the wall slope values is shown in Table 3.

These wall values are incorporated into the relations for surface shear stress and surface heat transfer rates in the next section, where contrasts are brought out between properties based on mixture of gases and the results based on the fundamental properties estimated from molecular dynamics for gold-water nanofluids.

### **SURFACE HEAT TRANSFER RATE**

The heat transfer rate from (1), with the use of the volume fraction in the diffusion

current relation and evaluated at the surface, (denoted by subscript  $w$ ) is

$$q_w = - \left[ k \frac{\partial T}{\partial y} + \rho_p D \frac{\partial \phi}{\partial y} h_p \right]_w \quad \text{eq. (27)}$$

The surface heat transfer rate here consists of thermal conduction, denoted by

$q_{w,C} = - (k \partial T / \partial y)_w$ ; the surface heat transfer rate due to the transport of thermal energy (

$h_p = c_p T$ ) by the diffusion current is denoted by  $q_{w,D} = - (\rho_p h_p D \partial \phi / \partial y)_w$ . It was shown that

the nonuniformity of the nanofluid volume fraction distribution has an effect on the temperature profile near the wall and on the thermal conductivity, i.e., the volume fraction diffusion effect also has an impact on the surface heat transfer rate due to thermal conduction.

Using the similarity transformation (13), the  $y$ -derivatives are recast into  $\eta$ -derivatives and through the normalization by the surface heat transfer for the base fluid, the

normalized conduction heat transfer rate becomes

$$q_{W,C}^* \equiv q_{W,C} / q_{W,f} = 1 + \phi_\infty \left[ (k^*)'_{\phi=0} + \theta_1'(0; Pr_f, Sc_f) / \theta_0'(0; Pr_f) \right]$$

eq. (28)

The dimensionless surface heat transfer rate is denoted by  $q_{W,C}^*$ . The dependence of the first

order temperature perturbation  $\theta_1(\eta; Pr_f, Sc_f)$  on the Schmidt number is indicated by its

differential equation (19). A correlation of  $\theta_1'(0)$  in terms of  $Pr_f, Sc_f$  is not available as

$\theta_0'(0; Pr)$ , which is obtained by Pohlhausen [21] and given by (22). The similarity behavior of

the first order problem, in the Blasius sense, enabled the canceling out of the  $X^{1/2}$  factor in

the enhanced surface heat transfer relation upon normalization by  $q_{W,f}$ .

The surface heat transfer rate due to diffusion effects, when normalized by  $q_{W,f}$  becomes

$$q_{W,D}^* \equiv q_{W,D} / q_{W,f} = \phi_\infty \rho_p^* c_p^* [(\Phi_W - 1) / (1 - T_\infty / T_W)] (Pr_f / Sc_f) \theta_1'(0) / \theta_0'(0)$$

eq. (29)

where the corresponding dimensionless surface heat transfer rate is defined as  $q_{W,D}^*$ . The ratio

$(Pr_f/Sc_f)$  is actually  $(Le_f)^{-1}$ , where  $Le_f$  is a Lewis number. In this definition, the factor  $\phi_\infty$ , which is the perturbation parameter in the present formulation, is removed from the denominator in Buongiorno's [13] definition. In view of the correlations from numerical solution result, (22) and (25), for Prandtl and Schmidt number ranges appropriate to the

present problem ( $Pr_f = 7$ ,  $Sc_f \cong 2 \times 10^4$ ), eq. (29) becomes

$$q_{W,D}^* = q_{W,D} / q_{W,f} = \phi_\infty \rho_p^* c_p^* [(\Phi_W - 1) / (1 - T_\infty / T_W)] 1.02 (Le_f)^{-2/3} \quad \text{eq. (30)}$$

To interpret the diffusion transport of thermal energy effect on surface heat transfer rate, first,

the normalizing base fluid convective-conduction heat transfer rate is positive,  $q_{W,f} > 0$  if

$T_W > T_\infty$ ; i.e., the hotter wall loses heat to the cooler freestream. This situation is retained in

the following discussion. The diffusion heat flux, on the other hand, even if  $T_W > T_\infty$  in eq.

(30), depends on the sign of  $(\Phi_W - 1)$ . If  $\Phi_W < 1$ , there is a depletion of nanofluid concentration at the wall and the diffusion current would be towards the wall and there

negative, thus rendering  $q_{W,D} / q_{W,f} < 0$ . On the other hand, if there is a surplus of nanofluid

concentration near the wall,  $\Phi_W > 1$ , the diffusion current is directed away from the wall and

$$q_{W,D} / q_{W,f} > 0$$

eq. (30) indicates . Thus, heat is transferred away from the wall by the diffusion current and thus the nanofluid conduction enhancement given by eq. (28) is augmented by the nanoparticle diffusion transport effect given by eq. (30).

In the first order perturbation, the enhancement is a linear function of  $\phi_\infty$ , it is instructive to obtain the numerical values of the slope of the corresponding rates at the origin

of  $\phi_\infty = 0$ , [reminiscent of the thermophysical properties (7)-(10)]. In dimensionless form, the surface heat transfer rates are recast as

$$(q_{W,C}^* - 1) / \phi_\infty = (q_{W,C}^*)'_{\phi=0} + (q_{W,D}^*)'_{\phi=0} \quad \text{eq. (31)}$$

where  $q_{W,C}^* = q_{W,C} / q_{W,f}$ , the dimensionless form of eq. (27), and the slopes at the origin of the volume fraction are obtained from the right hand sides of eqs. (28) and (30), respectively.

$$(q_{W,C}^*)'_{\phi=0} = \left[ (k^*)'_{\phi=0} + \theta_1'(0; \text{Pr}_f, \text{Sc}_f) / \theta_0'(0; \text{Pr}_f) \right] \quad \text{eq. (32)}$$

$$(q_{W,D}^*)'_{\phi=0} = \rho_p^* c_{p,l}^* [(\Phi_W - 1) / (1 - T_\infty / T_W)] 1.02 (Le_f)^{-2/3} \quad \text{eq. (33)}$$

recalling primes associated with the sub-designations  $\phi = 0$ , such as  $(q_{W,C}^*)'_{\phi=0}$  and  $(k^*)'_{\phi=0}$ ,

indicate differentiation with respect to  $\phi$ , whereas primes associated with boundary layer

functions indicate differentiation with respect to  $\eta$ .

Because of the large Lewis numbers encountered (which will decrease as the average

nanoparticle diameters increase), it is expected that  $(q_{W,D}^*)'_{\phi=0} \ll (q_{W,C}^*)'_{\phi=0}$ , for reasonable

$T_w/T_\infty$  values. Thus, the direct thermal energy transfer by the diffusion current as a contribution to surface heat transfer rates, is relatively small. However, the steep variation of the concentration profiles near the wall has a much greater impact on the wall values of the first order temperature perturbation.

The results in Tables 1 through 3 show considerable influence of the steep

concentration diffusion layer on the first order heat transfer parameter,  $\theta_1'(0)$ . To best

illustrate this, the parameter  $\theta_1'(0)$  under the influence of the steep diffusion layer is normalized by that the “insulated” zero-flux solid wall concentration layer [12].

The effect of the diffusion layer on  $\theta_1'(0)$  is normalized by the case in which there is no variation of concentration across the boundary layer reflected by the middle column. The

diffusional layer effect is thus compared to unity. The results are for  $Pr_f = 7, Sc_f = 2 \times 10^4$  as

depicted by the profiles in Figures 2 through 10. In the case for depletion of concentration at the wall, Figure 3 shows that the first order temperature profile is reversed, caused by the steep diffusion layer, where the diffusion flux is pointed inwards into the boundary layer compared to that when there is no diffusion layer (Figure 2). The impact of the diffusion

layer on  $\theta_1(\eta)$  can be traced to eq. (19). Because of the large  $Sc_f$  the last term in eq. (19), which is due to the transport of thermal energy by the diffusion currents, is much less important than the strong effect of the steep diffusion layer near the wall. This is because of

the strong dependence of the thermal conductivity on the steep gradient  $\Phi'(\eta)$  near the wall

as depicted in Figures 3, 4 as well as 5,7 and 9,10 for the boundary condition  $\Phi(0)=0$

(withdrawing concentration into the wall) and  $\Phi(0)=2$  (supplying concentration from the wall).

In summary, the surface heat transfer rate for  $Sc_f \gg 1$  in the present of diffusion layer is approximated by

$$q_w^* \cong 1 + \phi_\infty (q_{w,c}^*)'_{\phi=0} + \mathcal{O}(10^{-3}) \tag{eq. (34)}$$

where  $(q_{w,c}^*)'_{\phi=0}$  is given in eq. (32). The expression (32) provide the distinct mechanism due

to thermal conduction enhancement,  $(K^*)'_{\phi=0}$ , and the modification due to convective heat

transfer effect of steep diffusion layer (for  $\Phi(0) = 0, 2$ ) on the values of  $\theta_1'(0)/\theta_0'(0)$  (see

Tables 1-3, where  $\theta_0'(0)$  is given by eq. (22).

The surface heat transfer rate results for the three boundary conditions on the volume concentration are indicated in Table 4. The condition is where the porous matrix wall has the wall concentration removed to zero volume fraction. in which case the diffusion current is directed towards the wall. The zero-volume flux at a solid wall is indicated by the , which produces the same result when is imposed [12]. In this case, the freestream concentration is maintained throughout the boundary layer and there is no diffusional effect. The case is where the volume concentration at the wall is maintained to be twice that of the freestream value, the diffusional current is directed towards the outer regions of the boundary layer. Arrows placed next to the slope indicate whether it increased or decreased compared to the zero-diffusion case of for the nanofluid in question.

Table 5 is constructed for the shear stress in the next section.

## **SHEAR STRESS**

The shear stress on the wall is

$$\tau_w = \left( \mu \frac{\partial u}{\partial y} \right)_w = \mu_f U \sqrt{\frac{U}{\nu_f X}} \mu_w^* f''(0)$$

eq. (35)

$$\tau_{W,f} = \mu_f U \sqrt{U / \nu_f} \chi f_0''(0)$$

The base fluid shear stress at the wall is . Using the perturbation expansion of the form eq. (12) and the representation of the dynamic viscosity given by eq. (9). The dimensionless shear stress is

$$\tau_W^* = \tau_W / \tau_{W,f} = 1 + \phi_\infty [(\mu^*)'_{\phi=0} + f_1''(0) / f_0''(0)] \quad \text{eq. (36)}$$

where a slope is similarly defined as

$$\text{eq. (37)}$$

The representation is similar to that for the dimensionless surface heat transfer rate. No representation in terms of the skin friction coefficient is made, as this introduces extraneous volume fractions associated with the free stream density. The results are summarized in Table 5 (arrows are placed next to the slopes , to indicate whether they increased or decreased compared to the zero-diffusion case of ).

## CONCLUSIONS

The effects of nonuniformities of the nanoparticle volume fraction in the boundary layer are the subjects of the present work. Owing to the large Schmidt number, the direct effect of diffusional transport of thermal energy has a negligible impact on the surface heat transfer rate. However, the volume fraction non-uniformities have an impact on both the nanofluid velocity and temperature profiles near the wall, thus affecting in no small way the conduction surface heat transfer rate. The illustrative cases considered is the complete depletion of the volume concentration at the wall, i.e., the free stream volume fraction is reduced to zero at the wall ; the other contrasting condition is that the freestream volume fraction value is doubled at the wall . The results of these cases are compared to the zero-flux at a solid wall for which . Using the physically more reliable molecular dynamics estimates of thermophysical properties for gold-water nanofluid [4, 21, 22] for the present discussion,

the surface heat transfer rate enhancement, from Table 4, is 2.4 times that of the uniform concentration case (case 3). In magnitude estimates, the enhancement is about 2.4 at  $\phi = 0.01$ . In this case, the skin friction rise (from Table 5) is 1.2. The value is about the same as that for the uniform concentration case [12]. One can somewhat boldly generalize that if the nanofluid volume concentration is lowered from that in the freestream, perhaps by a porous matrix wall, then through the influence of the very thin concentration layer, the nanofluid velocity and temperature profiles are so modified, though the dependence of the transport properties on concentration, that the surface heat transfer rate could be significantly increased and skin friction rise decreased, much contrary to the pessimistic conclusion about nanofluids raised by Venerus et al. [6].

Gold-water heat transfer experiments in gold-water nanofluid are recently reported by Sabir et al. [24]. Their reported surface heat transfer rate enhancement is much more spectacular than that owing to thermal conductivities obtainable from field theories (e.g., Maxwell [7], Rayleigh [8] and their modifications [5]) and that owing to convective heat transfer of dilute concentration of nanofluids considered here and elsewhere [12]. Thus, further consideration of these results [24] is delayed until a better understanding of the nature of their nanofluid and method of measurements could be attained.

An important assumption in boundary layer studies is that the freestream quantities are taken as uniform, and this permitted the similarity considerations possible. Measurements in micro-channels and tubes [9, 10], which are fed by tubes at the leading edge, for sure renders the oncoming freestream quantities nonuniform. As such, similar solutions are difficult to obtain. The importance of micro-channel and tube measurements bring out the importance of the leading edge or entrance region, in which case, the boundary layer is used to approximate the entrance region [11, 12] before the freestream is affected downstream

towards the developed region. In this situation, the boundary layer may well be worthy of careful measurements in a nanofluid. It would thus not be necessary to use micro-channels for measurements as the freestream in the boundary layer situation is unconfined and uniform. One could think of the initial boundary layer experiments in nanofluid channel where appropriately instrumented experiments could be carried out. We point to the nanofluid perturbation velocity and temperature profiles, that is, the difference between such profiles in a nanofluid and those separately measured in the base fluid.

## ***NOMENCLATURE***

$C$   
nanofluid heat capacity [J/K]

$C_f$   
basefluid heat capacity [J/K]

$C_p$   
nanoparticle heat capacity [J/K]

$C_f$   
skin friction coefficient

$D$   
Brownian diffusion coefficient [m<sup>2</sup>/s]

$f$   
dimensionless, similarity stream function

$h$   
nanofluid static enthalpy [J]

$h_p$   
static enthalpy of nanoparticles [J]

nanoparticle phase diffusion

$k$   
thermal conductivity [W/m·K]

$k_B$   
Boltzmann number [J/K]

$L$   
physical length scale [m]

, Lewis number

, Prandtl number

$q$   
heat transfer rate [W/m<sup>2</sup>.s]

$Q$   
any physical quantity

$r_d$   
nanoparticle radius [m]

, Reynolds number

$Sc_f = \nu_f / D$   
, Schmidt number

$T$   
absolute temperature [K]

$u, v$   
stream wise and normal-to-wall velocity components [m/s]

$U$  velocity of the fluid [m/s]

$x, y$   
streamwise and normal-to-wall coordinates

$x_p$   
nanoparticle phase mass fraction

### ***Greek Symbols***

similarity independent variable

$\delta$  diffusion layer

$\xi$

$\psi$  stream function

$\theta = (T - T_\infty)/(T_w - T_\infty)$ , dimensionless temperature

thermal diffusivity [m<sup>2</sup>/s]

$\mu$   
dynamic viscosity [N·s/m<sup>2</sup>]

kinematic viscosity [m<sup>2</sup>/s]

nanofluid density [kg/m<sup>3</sup>]

$\rho_p$   
nanoparticle density [kg/m<sup>3</sup>]

$\rho_f$   
base fluid density [kg/m<sup>3</sup>]

$\tau$   
shear stress [N/m<sup>2</sup>]

$\phi$   
nanoparticle phase volume fraction

, normalized volume concentration

### ***Subscripts***

C pertaining to thermal conduction

pertaining to Brownian diffusion

base fluid

nanoparticle

evaluated at the wall

$\infty$  evaluated at the fluid

at

zeroth order perturbation (the base fluid)

1 first order perturbation

mix mixture

MD molecular dynamics

### ***Superscripts***

\* dimensionless

## REFERENCES

- [1] Choi, S. U. S., Enhancing Thermal Conductivity of Fluids with Nanoparticles, in *Developments and Applications of Non-Newtonian Flows*, eds. D. A. Siginer and H. P. Wang, pp 99-105, FED-Vol. 231/MD-Vol. 66, American Society of Mechanical Engineers, New York, 1995.
- [2] Das, S. K., Choi, S. U. S., Yu, W., and Pradeep, T., *Nanofluid Science and Technology*, Wiley, Hoboken, N. J., 2008.
- [3] Das, S. K., Choi, S. U. S., and Patel, H. E., Heat Transfer in Nanofluids—A Review, *Heat Transfer Engineering*, vol.27, no. 10, pp. 3-18, 2006.
- [4] Paolucci, S., and Pulliti, G., Properties of Nanofluids, in *Heat Transfer Enhancement with Nanofluids*, eds. V. Bianco, O. Manca, S. Nardini, and K. Vafai, pp.1-44, CRC Press, New York, 2015.
- [5] Buongiorno, J., Venerus D.C., Prabhat N., McKrell T., Townsend J., Christianson R., Tolmachev Y. V., Keblinski P., Hu L.-W., Alvarado J. L., Bang I.-C., Bishnoi S. W., Bonetti M., Botz F., Cecere A., Chang Y., Chen G., Chen H., Chung S. J., Chyu M. K., Das S. K., Paola R., Ding Y., Dubois F., Dzido G., Eapen J., Escher W., Funfschilling D., Galand Q., Gao J., Gharagozloo P. E., Goodson K. E., Gutierrez J. G., Hong H., Horton M., Hwang K. S., Iorio C. S., Jang S. P., Jarzebski A. B., Jiang Y., Jin L., Kabelac S., Kamath A., Kedzierski M. A., Kieng L. G., Kim C., Kim J.-H., Kim S., Lee S.H., Leong K. C., Manna I., Michel B., Ni R., Patel H. E., Philip J., Poulikakos D., Reynaud C., Savino R., Singh P. K., Song P., Sundararajan T., Timofeev E., Triticak T.,

- Turanov A. N., Vaerenbergh S. V., Wen D., Witharana S., Yang C., Yeh W.-H., Zhao X.-Z. and Zhou S.-Q., A Benchmark Study on the Thermal Conductivity of Nanofluids, *Journal of Applied Physics*, vol.106, no. 9, pp. 094312-1 – 094312-14, 2009.
- [6] Venerus, D. C., Buongiorno, J., Christianson R., Townsend J., Bang I.-C., Chen G., Chung S. J., Chyu M. K., Chen H., Ding Y., Dubois F., Dzido G., Funf-schilling D., Galand Q., Gao J., Hong H., Horton M., Hu L.-W., Iorio C. S., Jarzebski A. B., Jiang Y., Kabelac S., Kedzierski M. A., Kim C., Kim J.-H., Kim S., McKrell T., Ni R., Philip J., Prabhat N., Song P., Vaerenbergh S. V., Wen D., Witharana S., Zhao X.-Z., and Zhou S.-Q., Viscosity Measurements on Colloidal Dispersions (Nanofluids) for Heat Transfer Applications, *Applied Rheology*, vol. 20, no. 4, pp. 44582-1 – 44582-7, 2010.
- [7] Maxwell, J. C. *A Treatise on Electricity and Magnetism*, vol. 1, Clarendon Press, Oxford, 1873.
- [8] Rayleigh, On the Influence of Obstacles Arranged in Rectangular Order upon Properties of a Medium, *Philosophical Magazine*, vol.34, no. 211, pp. 481-502, 1892.
- [9] Wen, D., and Ding, Y., Experimental Investigation into Convective Heat Transfer of Nanofluids at the Entrance Region under Laminar Flow Conditions, *International Journal of Heat and Mass Transfer*, vol. 47, no. 24, pp. 5181-5188, 2004
- [10] Jung, J.-Y., Oh, H.-S., and Kwak, H.-Y., Forced Convection of Nanofluids in Microchannels, *International Journal of Heat and Mass Transfer*, vol. 52, nos. 1-2, pp. 466-472, 2009.
- [11] Liu, J. T. C., On the Anomalous Laminar Heat Transfer Intensification in Developing Region of Nanofluid Flow in Channels or Tubes, *Proceedings of the Royal Society A*, vol. 468, pp. 2398-2383, 2012
- [12] Liu, J. T. C., Fuller, M. E., Wu, K. L., Czulak, A., Kithes, A. G., and Felton, C. J., Nanofluid Flow and Heat Transfer in Boundary Layers at Small Nanoparticle Volume

- Fraction: Zero nanoparticle Flux at Solid Wall, *Archives of Mechanics*, vol. 68, pp. 75-100, Warszawa, 2017.
- [13] Buongiorno, J., Convective Transport in Nanofluids, *Journal of Applied Physics*, vol. 106, no. 3, pp. 240-250, 2006.
- [14] Einstein, A., On the motion of small particles suspended in liquids at rest required by the molecular-kinetic theory of heat. *Annalen der Physik*, vol. 17, pp. 549-560, 1905. (republication of 1926 translation, Dover Publications, Inc. 1956).
- [15] Pfautsch, E., Forced Convection in Nanofluids over a Flat Plate, M.Sc. thesis, University of Missouri, Columbia, MO, 2008.
- [16] Bird, R. B., Stewart, W. E., and Lightfoot, E. N. *Transport Phenomena*, 2<sup>nd</sup> ed., Wiley, Hoboken, N.J.
- [17] Probstein, R. F. *Physicochemical Hydrodynamics*, 2<sup>nd</sup> ed., Wiley, Hoboken, N. J., 1994.
- [18] Nield, D. A., and Kuznetsov, A. V., Modeling Convection in Nanofluids, in *Heat Transfer Enhancement with Nanofluids*, eds. V. Bianco, O. Manca, S. Nardini, and K. Vafai, pp. 325-340, CRC Press, New York, 2015.
- [19] Lees, L., Laminar Heat Transfer over Blunt-Nosed Bodies at Hypersonic Flight Speeds, *Jet Propulsion*, vol. 26, no. 4, pp. 259-269, p. 274, 1956.
- [20] Lagerstrom, P. A., *Laminar Flow Theory*, Princeton University Press, Princeton, N. J., 1996.
- [21] Schlichting, H., *Boundary Layer Theory*, 7<sup>th</sup> ed. (translated by J. Kestin), McGraw-Hill, N. Y., 1979.
- [22] Puliti, G., Properties of Gold-Nanofluid Nanofluids using Molecular Dynamics, Ph.D. thesis, University of Notre Dame, South Bend, IN., 2012.

[23] Puliti, G., Paolucci, S., and Sen, M., Thermodynamics Properties of Gold-Water Nanofluids using Molecular Dynamics, *Journal of Nanoparticle Research*, vol. 14, no. 12, article no. 1296.

[24] Sabir, R., Ramzan, N., Umer, A., Muryam, H., An experimental study of forced convection heat transfer characteristic of gold water nanofluid in laminar flow, *Sci. Int. (Lahore)*, 27, 235–241, 2015.

### **List of Tables**

Table 1. Alumina-water nanofluid (*mix*)

$\Phi(0)$	$\Phi'(0)$	$f_1''(0)$	$\theta_1'(0)$
0	9.2	-0.76	-2.36
1	0	0.65	1.30
2	-9.2	0.88	4.95

Table 2. Gold-water nanofluid (*mix*)

$\Phi(0)$	$\Phi'(0)$	$f_1''(0)$	$\theta_1'(0)$
0	9.2	1.79	-2.73
1	0	2.61	-0.92
2	-9.2	3.43	0.87

Table 3. Gold-water nanofluid (MD)

$\Phi(0)$	$\Phi'(0)$	$f_1''(0)$	$\theta_1'(0)$
0	9.2	-1.87	-8.2
1	0	1.44	3.94
2	-9.2	4.76	16.08

Table 4. Surface heat transfer rate

Table 5. Skin friction results:  $\tau_W^* = 1 + \phi_\infty [(\mu^*)'_{\phi=0} + f_1'(0) / f_0''(0)]$

	$(\mu^*)'_{\phi=0}$	$\Phi(0)=0:$		$\Phi'(0)=0:$		$\Phi(0)=2:$	
		$f_1''(0) / f_0''(0)$	$(\tau_W^*)'_{\phi=0}$	$f_1''(0) / f_0''(0)$	$(\tau_W^*)'_{\phi=0}$	$f_1''(0) / f_0''(0)$	$(\tau_W^*)'_{\phi=0}$
$Al_2O_3 - water]_{MIX}$	2.5	- 2.29	0.21↓	1.96	4.46	2.65	5.15↓
$Au - water]_{MIX}$	2.5	5.39	7.89↓	7.86	10.36	10.33	12.83↑
$Au - water]_{MD}$	10	- 5.55	4.34↓	4.33	14.33	14.34	24.34↑

**List of Figure captions**

Figure 1. The base fluid velocity and temperature profiles: The Blasius function:  $f_0'(\eta):$  \_\_\_\_\_, the Pohlhausen function  $\theta_0(\eta):$  - - - - - .  $Pr_f = 7.0$ .

Figure 2. First order perturbation functions, alumina-water nanofluid.  $\Phi(0; Sc_f) = 1$   
 $f_1'(\eta):$  \_\_\_\_\_,  $\theta_1(\eta; Pr_f):$  - - - - - ,  $\Phi(\eta; Sc_f):$ .....

$$\text{Pr}_f = 7, \text{Sc}_f = 2 \times 10^4$$

Figure 3a. The first order perturbation functions, alumina-water nanofluid.  $\Phi(0; \text{Sc}_f) = 0$

$$f_1(\eta): \text{-----}, \theta_1(\eta; \text{Pr}_f): \text{-----}, \Phi(\eta; \text{Sc}_f): \text{-----}$$

$$\text{Pr}_f = 7, \text{Sc}_f = 2 \times 10^4$$

Figure 3b. Wall region, alumina-water nanofluid.  $\Phi(0; \text{Sc}_f) = 0$

$$f_1(\eta): \text{-----}, \theta_1(\eta; \text{Pr}_f): \text{-----}, \Phi(\eta; \text{Sc}_f): \text{-----}$$

$$\text{Pr}_f = 7, \text{Sc}_f = 2 \times 10^4$$

Figure 4a. First order perturbation functions, alumina-water nanofluid.  $\Phi(0; \text{Sc}_f) = 2$

$$f_1(\eta): \text{-----}, \theta_1(\eta; \text{Pr}_f): \text{-----}, \Phi(\eta; \text{Sc}_f): \text{-----}$$

$$\text{Pr}_f = 7, \text{Sc}_f = 2 \times 10^4$$

Figure 4b. Wall region, alumina-water nanofluid.  $\Phi(0; \text{Sc}_f) = 2$

$$f_1(\eta): \text{-----}, \theta_1(\eta; \text{Pr}_f): \text{-----}, \Phi(\eta; \text{Sc}_f): \text{-----}$$

$$\text{Pr}_f = 7, \text{Sc}_f = 2 \times 10^4$$

Figure 5a. First order perturbation functions, gold-water nanofluid (mix.).  $\Phi(0; \text{Sc}_f) = 0$

$$f_1(\eta): \text{-----}, \theta_1(\eta; \text{Pr}_f): \text{-----}, \Phi(\eta; \text{Sc}_f): \text{-----}$$

$$\text{Pr}_f = 7, \text{Sc}_f = 2 \times 10^4$$

Figure 5b. Wall region, gold-water nanofluid (mix.).  $\Phi(0; \text{Sc}_f) = 0$

$$f_1(\eta): \text{-----}, \theta_1(\eta; \text{Pr}_f): \text{-----}, \Phi(\eta; \text{Sc}_f): \text{-----}$$

$$\text{Pr}_f = 7, \text{Sc}_f = 2 \times 10^4$$

Figure 6. First order perturbation functions, gold-water nanofluid (mix.).  $\Phi(0; \text{Sc}_f) = 1$

$$f_1(\eta): \text{-----}, \theta_1(\eta; \text{Pr}_f): \text{-----}, \Phi(\eta; \text{Sc}_f): \text{-----}$$

$$\text{Pr}_f = 7, \text{Sc}_f = 2 \times 10^4$$

Figure 7a. First order perturbation functions, gold-water nanofluid (mix.).  $\Phi(0; \text{Sc}_f) = 2$

$$f_1(\eta): \text{-----}, \theta_1(\eta; \text{Pr}_f): \text{-----}, \Phi(\eta; \text{Sc}_f): \text{-----}$$

$$\text{Pr}_f = 7, \text{Sc}_f = 2 \times 10^4$$

Figure 7b. Wall region, gold-water nanofluid (mix.).  $\Phi(0; \text{Sc}_f) = 2$

$$f_1(\eta): \text{-----}, \theta_1(\eta; \text{Pr}_f): \text{-----}, \Phi(\eta; \text{Sc}_f): \text{-----}$$

$$\text{Pr}_f = 7, \text{Sc}_f = 2 \times 10^4$$

Figure 8. First order perturbation functions, gold-water nanofluid (MD).  $\Phi(0; \text{Sc}_f) = 1$

$$f_1'(\eta): \text{-----}, \theta_1(\eta; \text{Pr}_f): - - - - - , \Phi(\eta; \text{Sc}_f): \text{.....}$$

$$\text{Pr}_f = 7, \text{Sc}_f = 2 \times 10^4$$

Figure 9a. First order perturbation functions, gold-water nanofluid (MD).  $\Phi(0; \text{Sc}_f) = 0$

$$f_1'(\eta): \text{-----}, \theta_1(\eta; \text{Pr}_f): - - - - - , \Phi(\eta; \text{Sc}_f): \text{.....}$$

$$\text{Pr}_f = 7, \text{Sc}_f = 2 \times 10^4$$

Figure 9b. Wall region, gold-water nanofluid (MD).  $\Phi(0; \text{Sc}_f) = 0$

$$f_1'(\eta): \text{-----}, \theta_1(\eta; \text{Pr}_f): - - - - - , \Phi(\eta; \text{Sc}_f): \text{.....}$$

$$\text{Pr}_f = 7, \text{Sc}_f = 2 \times 10^4$$

Figure 10a. First order perturbation functions, gold-water nanofluid (MD).  $\Phi(0; \text{Sc}_f) = 2$

$$f_1'(\eta): \text{-----}, \theta_1(\eta; \text{Pr}_f): - - - - - , \Phi(\eta; \text{Sc}_f): \text{.....}$$

$$\text{Pr}_f = 7, \text{Sc}_f = 2 \times 10^4$$

Figure 10b. Wall region, gold-water nanofluid (MD).  $\Phi(0; \text{Sc}_f) = 2$

$$f_1'(\eta): \text{-----}, \theta_1(\eta; \text{Pr}_f): - - - - - , \Phi(\eta; \text{Sc}_f): \text{.....}$$

$$\text{Pr}_f = 7, \text{Sc}_f = 2 \times 10^4$$

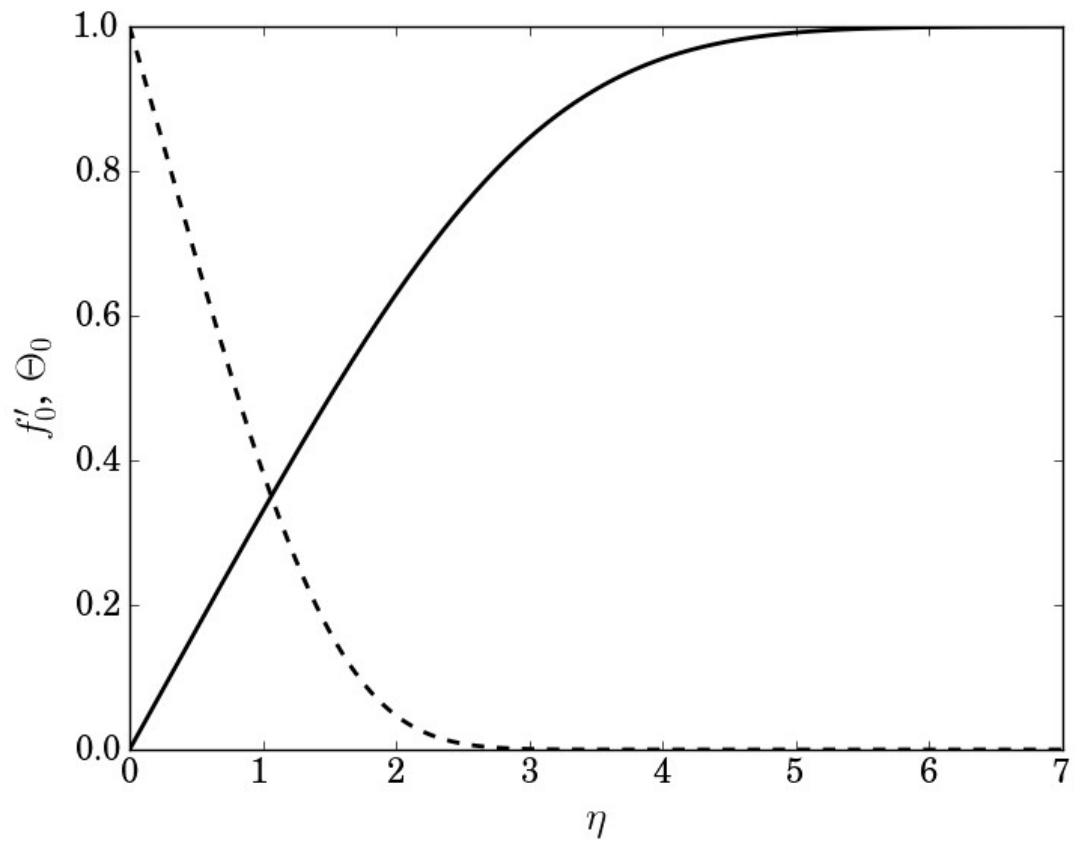
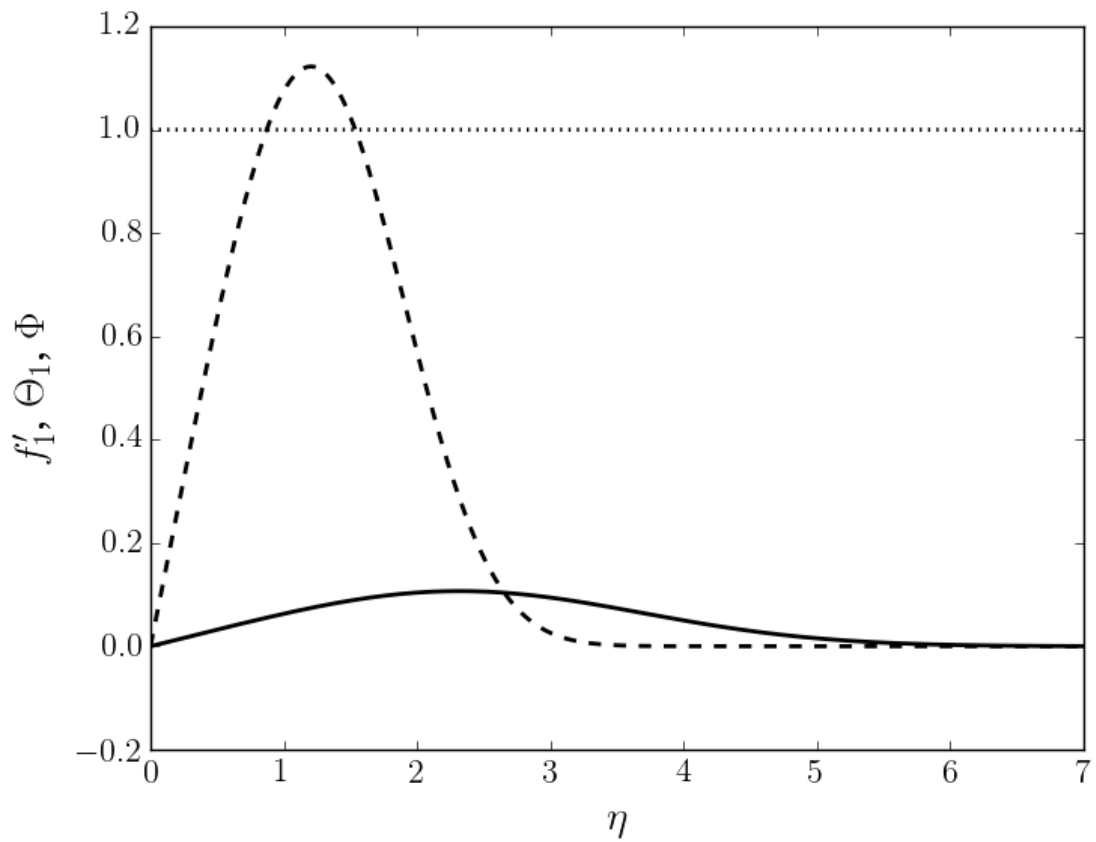
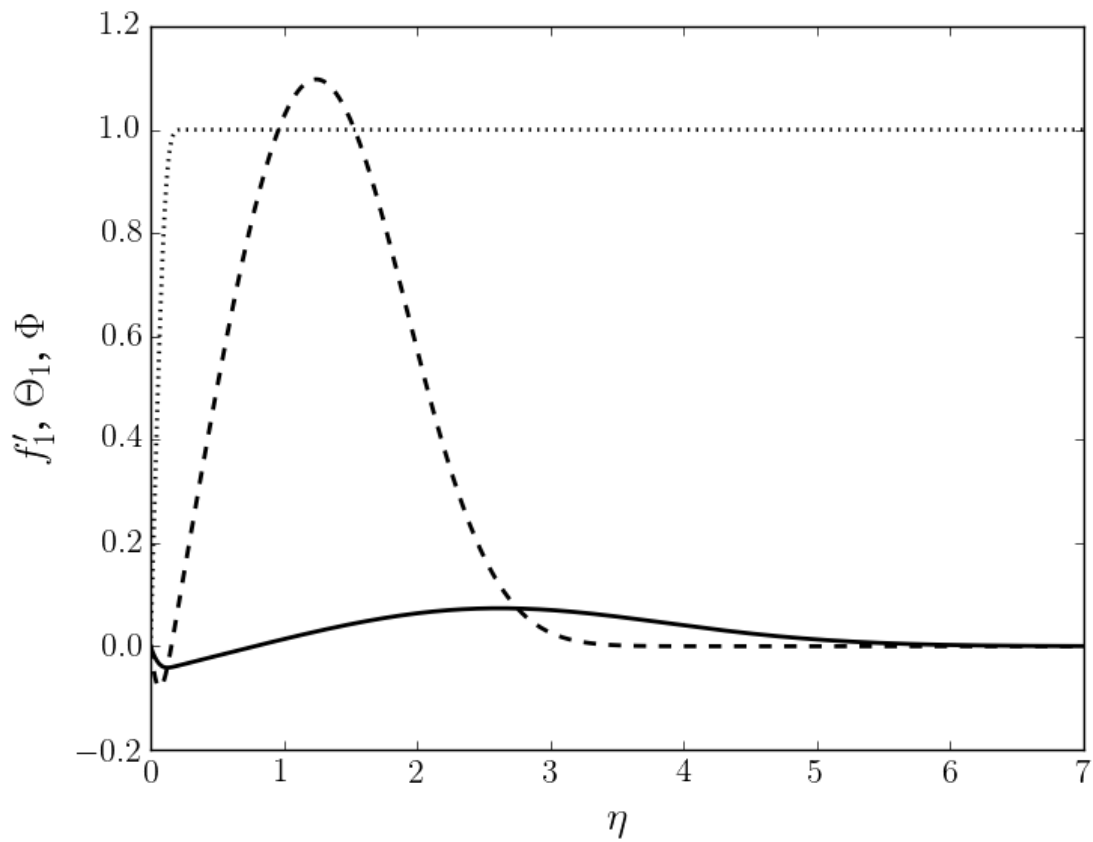


Figure 1. The base fluid velocity and temperature profiles: The Blasius function:  $f'_0(\eta)$ : —————, the Pohlhausen function  $\theta_0(\eta)$ : - - - - -  $Pr_f = 7.0$ .



**Figure 2.** First order perturbation functions, alumina-water nanofluid.  $\Phi(0; \mathcal{S}c_f) = 1$   
 $f'_1(\eta)$ : \_\_\_\_\_,  $\theta_1(\eta; Pr_f)$ : - - - - - ,  $\Phi(\eta; \mathcal{S}c_f)$ : .....  
 $Pr_f = 7$ ,  $\mathcal{S}c_f = 2 \times 10^4$



**Figure 3a.** The first order perturbation functions, alumina-water nanofluid.  $\Phi(0; \mathcal{S}c_f) = 0$   
 $f'_1(\eta)$ : \_\_\_\_\_,  $\theta_1(\eta; Pr_f)$ : - - - - - ,  $\Phi(\eta; \mathcal{S}c_f)$ : .....  
 $Pr_f = 7$ ,  $\mathcal{S}c_f = 2 \times 10^4$

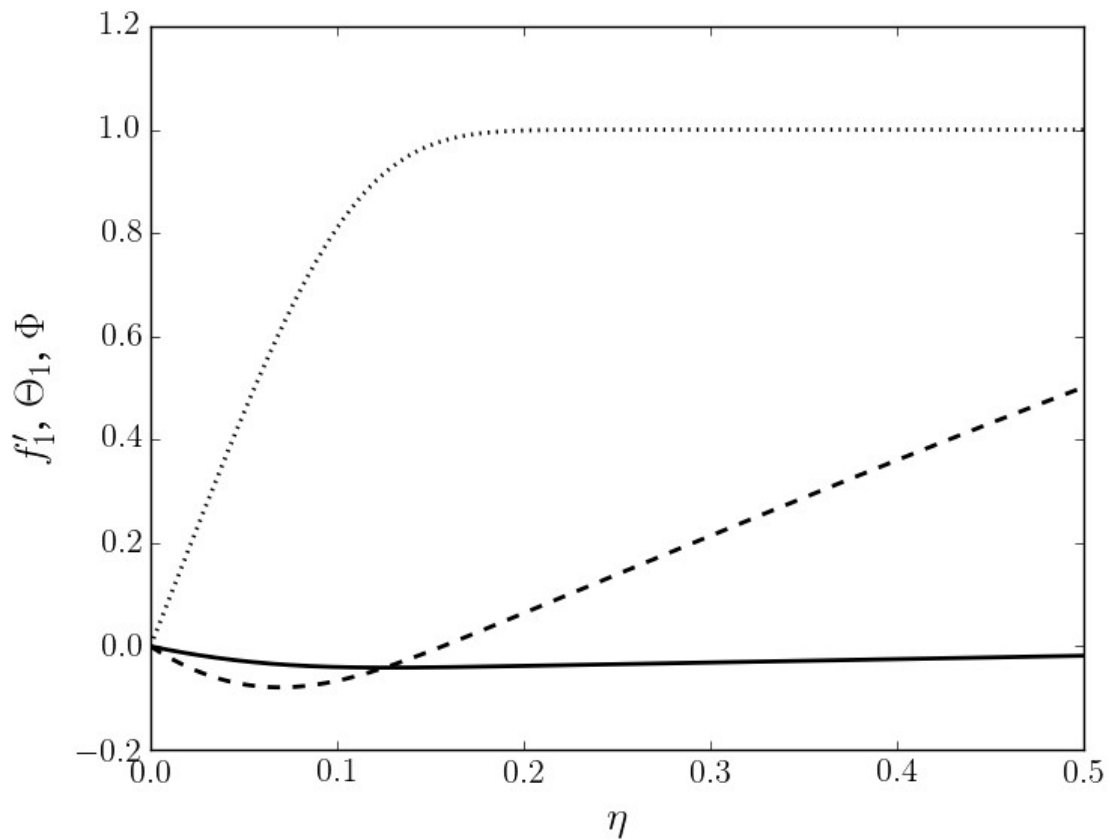


**Figure 3b.** Wall region, alumina-water nanofluid.  $\Phi(0; \text{Sc}_f) = 0$   
 $f_1'(\eta)$ : \_\_\_\_\_,  $\theta_1(\eta; \text{Pr}_f)$ : - - - - -,  $\Phi(\eta; \text{Sc}_f)$ : .....  
 $\text{Pr}_f = 7$ ,  $\text{Sc}_f = 2 \times 10^4$

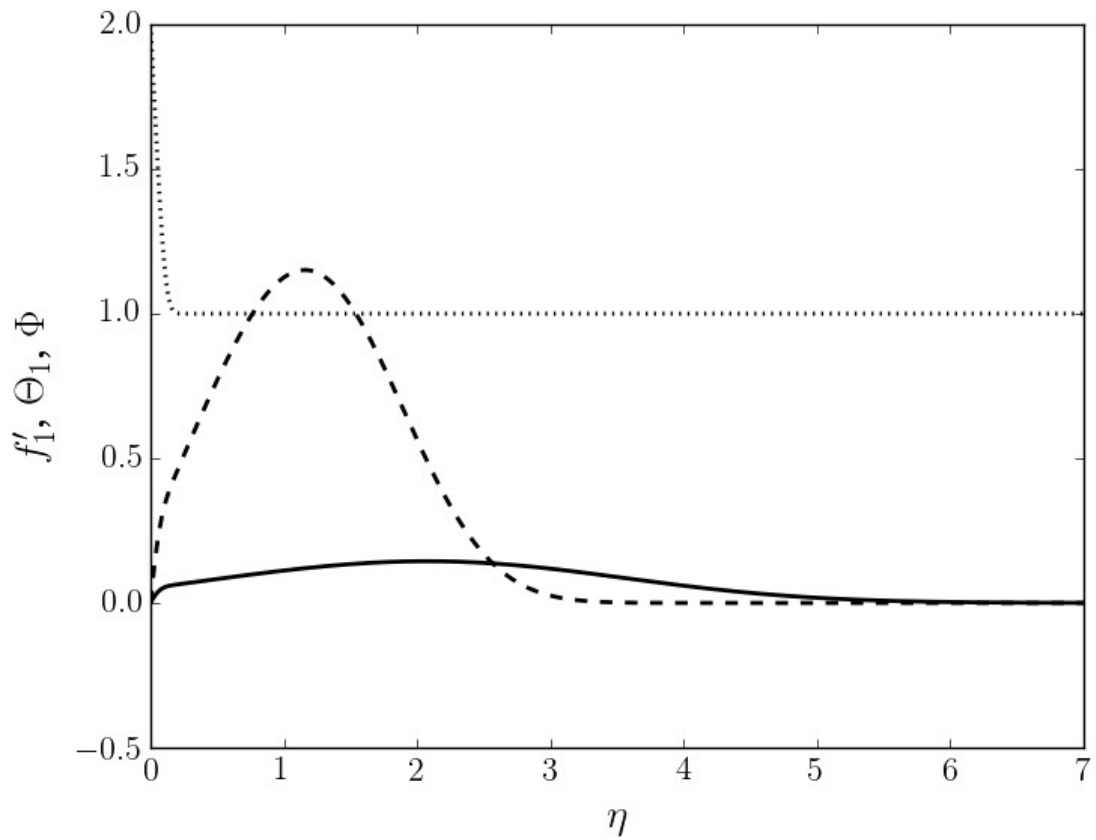


Figure 4a. First order perturbation functions, alumina-water nanofluid.  $\Phi(0; \mathcal{S}c_f) = 2$   
 $f'_1(\eta)$ : \_\_\_\_\_,  $\theta_1(\eta; Pr_f)$ : - - - - - ,  $\Phi(\eta; \mathcal{S}c_f)$ : .....  
 $Pr_f = 7$ ,  $\mathcal{S}c_f = 2 \times 10^4$

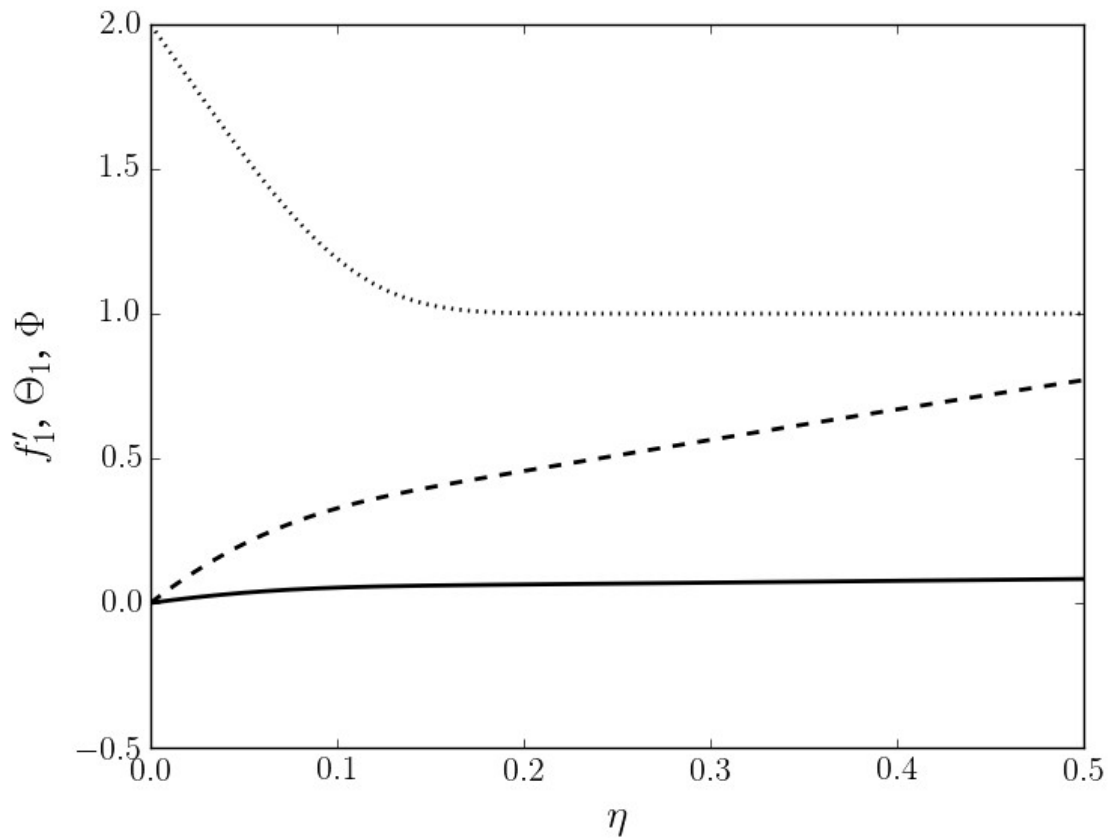


Figure 4b. Wall region, alumina-water nanofluent.  $\Phi(0; Sc_f) = 2$   
 $f'_1(\eta)$ : \_\_\_\_\_,  $\theta_1(\eta; Pr_f)$ : - - - - - ,  $\Phi(\eta; Sc_f)$ : .....  
 $Pr_f = 7$ ,  $Sc_f = 2 \times 10^4$

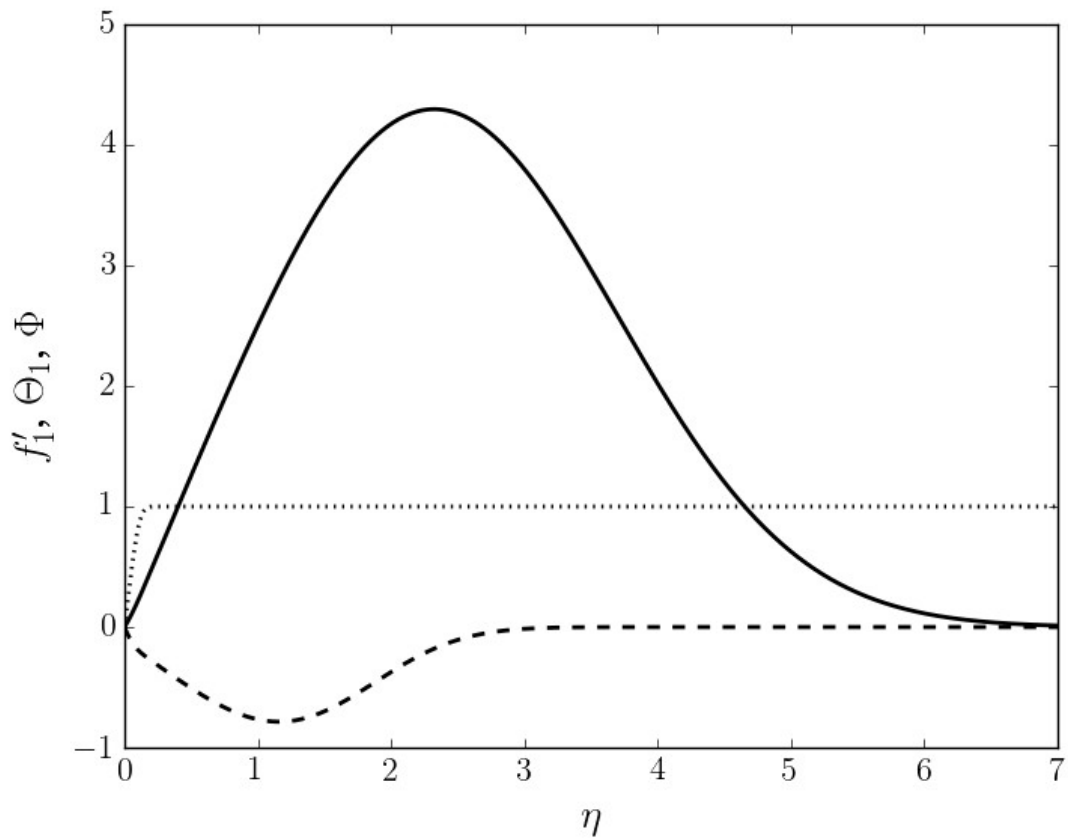


Figure 5a. First order perturbation functions, gold-water nanoffluid (mix.).  $\Phi(0; \mathbf{Sc}_f) = 0$   
 $f'_1(\eta)$ : \_\_\_\_\_,  $\theta_1(\eta; \text{Pr}_f)$ : - - - - - ,  $\Phi(\eta; \mathbf{Sc}_f)$ : .....  
 $\text{Pr}_f = 7$ ,  $\mathbf{Sc}_f = 2 \times 10^4$

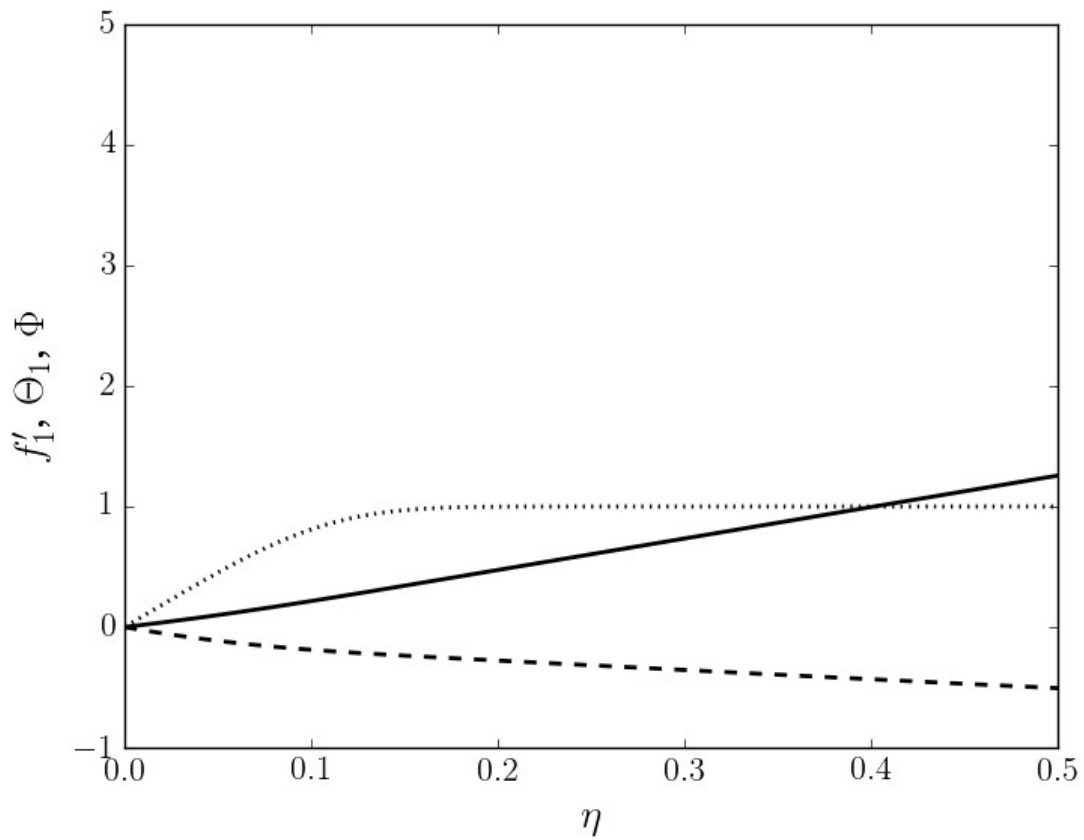


Figure 5b. Wall region, gold-water nanofluid (mix.).  $\Phi(0; \mathcal{SC}_f) = 0$   
 $f_1'(\eta)$ : \_\_\_\_\_,  $\theta_1(\eta; \text{Pr}_f)$ : - - - - - ,  $\Phi(\eta; \mathcal{SC}_f)$ : .....  
 $\text{Pr}_f = 7$ ,  $\mathcal{SC}_f = 2 \times 10^4$

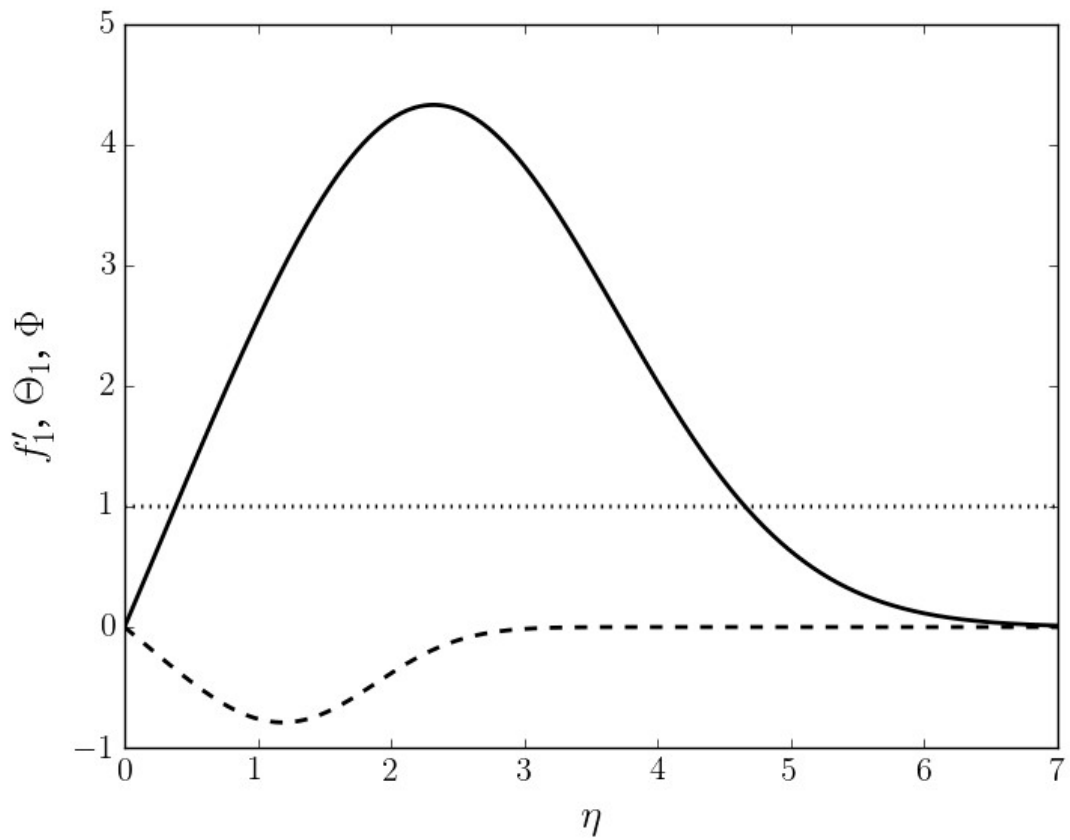


Figure 6. First order perturbation functions, gold-water nanofluid (mix.).  $\Phi(0; \mathcal{S}c_f) = 1$   
 $f'_1(\eta)$ : —————,  $\theta_1(\eta; Pr_f)$ : - - - - - ,  $\Phi(\eta; \mathcal{S}c_f)$ : .....  
 $Pr_f = 7$ ,  $\mathcal{S}c_f = 2 \times 10^4$

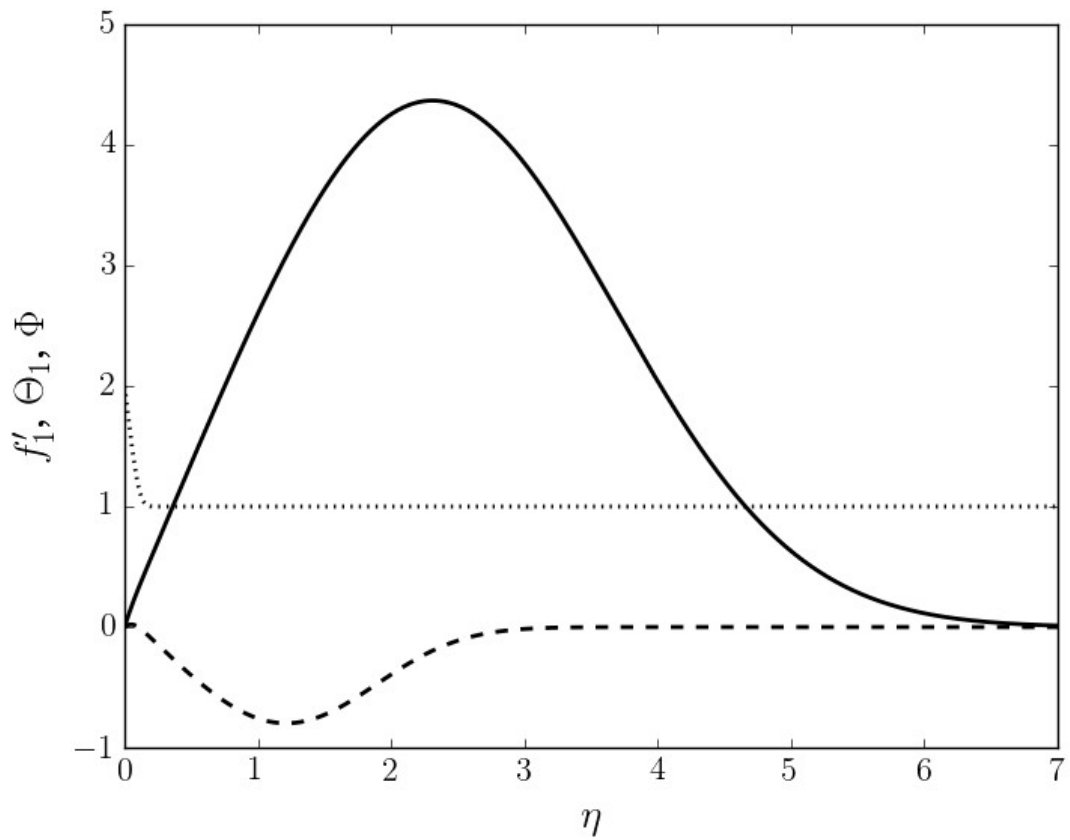


Figure 7a. First order perturbation functions, gold-water nanoffluid (mix.).  $\Phi(0; \mathcal{S}c_f) = 2$   
 $f_1'(\eta)$ : \_\_\_\_\_,  $\theta_1(\eta; Pr_f)$ : - - - - - ,  $\Phi(\eta; \mathcal{S}c_f)$ : .....  
 $Pr_f = 7$ ,  $\mathcal{S}c_f = 2 \times 10^4$

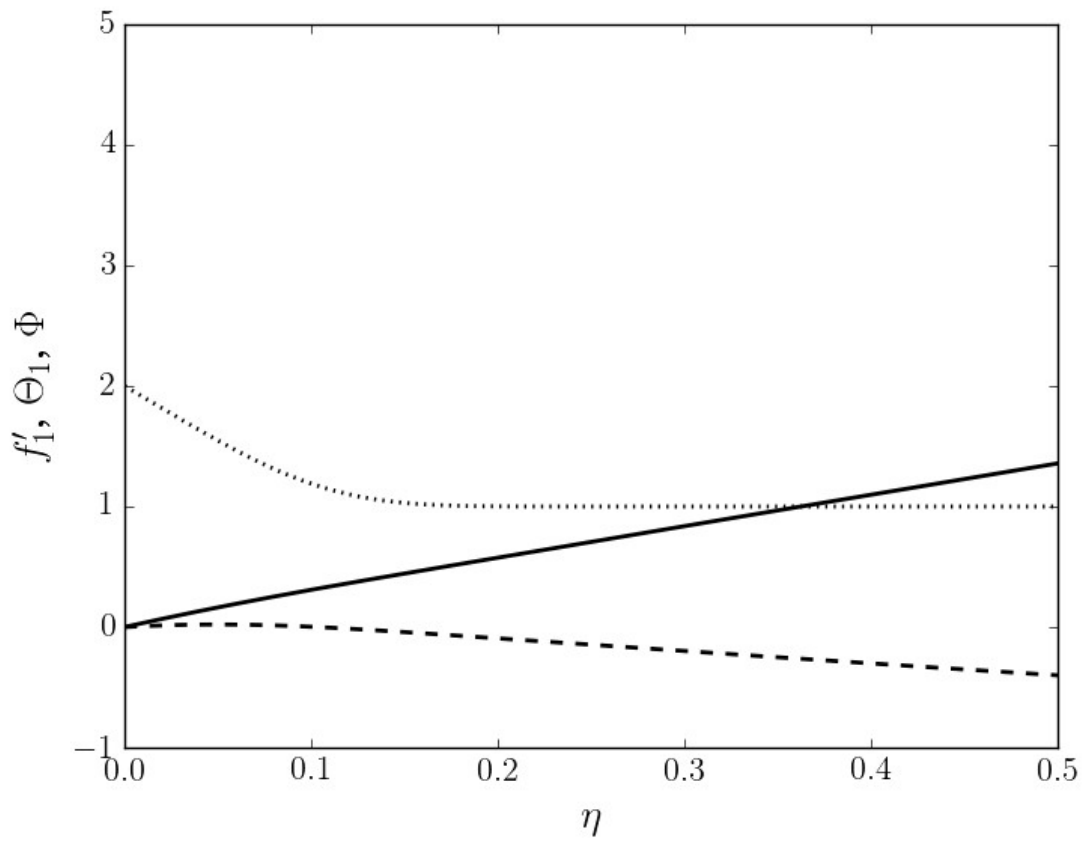
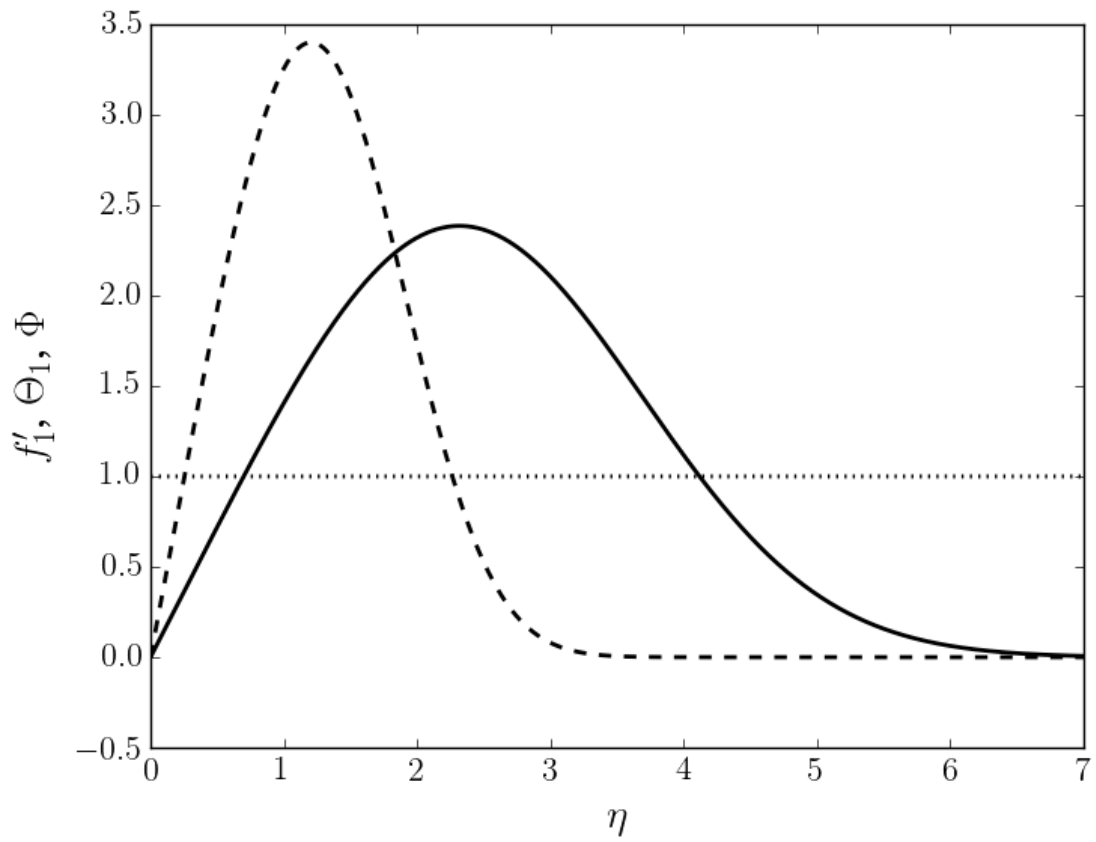
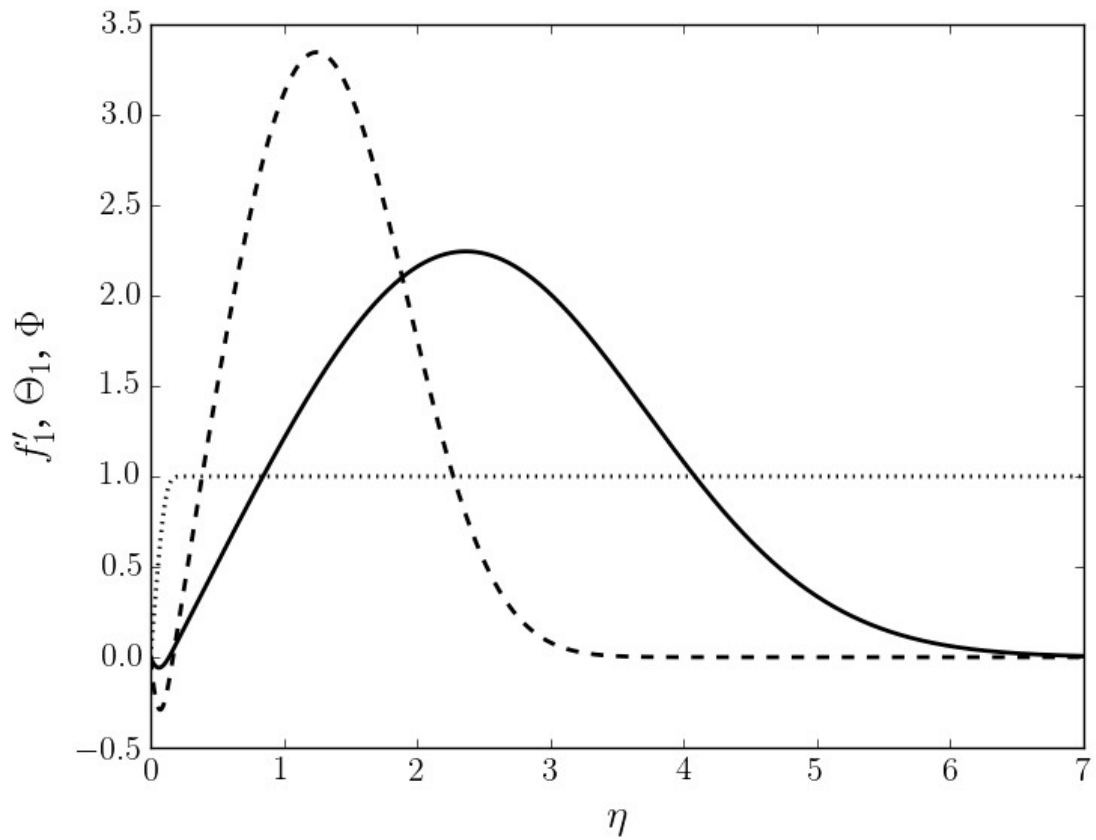


Figure 7b. Wall region, gold-water nanofluid (mix.).  $\Phi(0; Sc_f) = 2$   
 $f_1'(\eta)$ : \_\_\_\_\_,  $\theta_1(\eta; Pr_f)$ : - - - - - ,  $\Phi(\eta; Sc_f)$ : .....  
 $Pr_f = 7$ ,  $Sc_f = 2 \times 10^4$



**Figure 8.** First order perturbation functions, gold-water nanofluid (MD).  $\Phi(0; \mathbf{Sc}_f) = 1$   
 $f'_1(\eta)$ : \_\_\_\_\_,  $\theta_1(\eta; \text{Pr}_f)$ : - - - - - ,  $\Phi(\eta; \mathbf{Sc}_f)$ : .....  
 $\text{Pr}_f = 7$ ,  $\mathbf{Sc}_f = 2 \times 10^4$



**Figure 9a.** First order perturbation functions, gold-water nanofluid (MD).  $\Phi(0; \mathcal{S}c_f) = 0$   
 $f'_1(\eta)$ : \_\_\_\_\_,  $\theta_1(\eta; Pr_f)$ : - - - - - ,  $\Phi(\eta; \mathcal{S}c_f)$ : .....  
 $Pr_f = 7$ ,  $\mathcal{S}c_f = 2 \times 10^4$

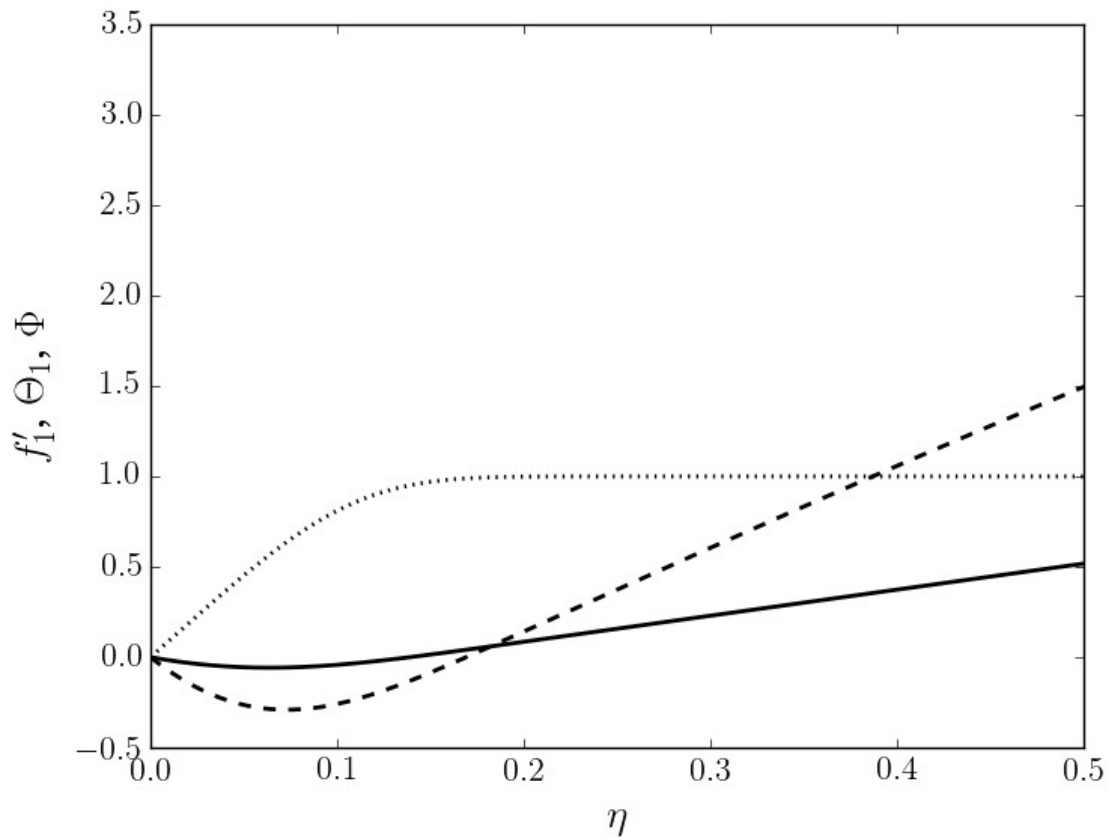


**Figure 9b.** Wall region, gold-water nanofluid (MD).  $\Phi(0; Sc_f) = 0$   
 $f'_1(\eta)$ : \_\_\_\_\_,  $\theta_1(\eta; Pr_f)$ : - - - - -,  $\Phi(\eta; Sc_f)$ : .....  
 $Pr_f = 7$ ,  $Sc_f = 2 \times 10^4$

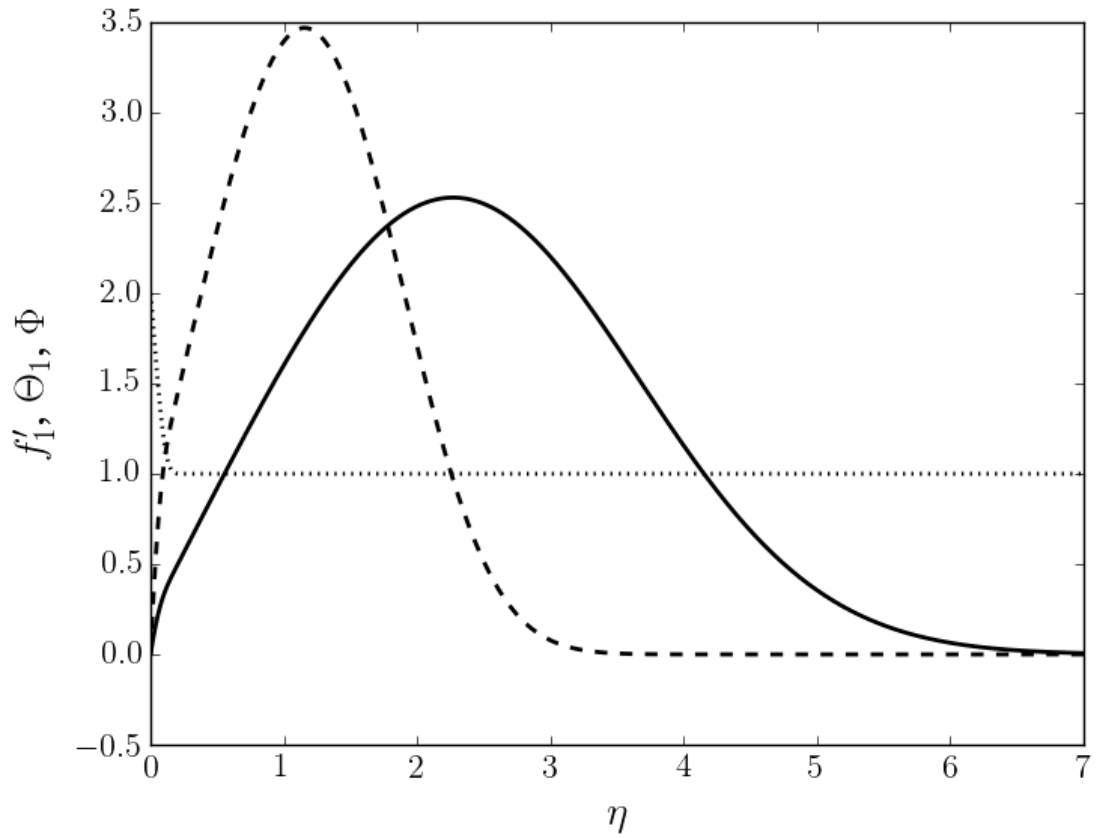


Figure 10a. First order perturbation functions, gold-water nanofluid (MD).  $\Phi(0; \mathcal{S}c_f) = 2$   
 $f'_1(\eta)$ : \_\_\_\_\_,  $\theta_1(\eta; Pr_f)$ : - - - - - ,  $\Phi(\eta; \mathcal{S}c_f)$ : .....  
 $Pr_f = 7$ ,  $\mathcal{S}c_f = 2 \times 10^4$

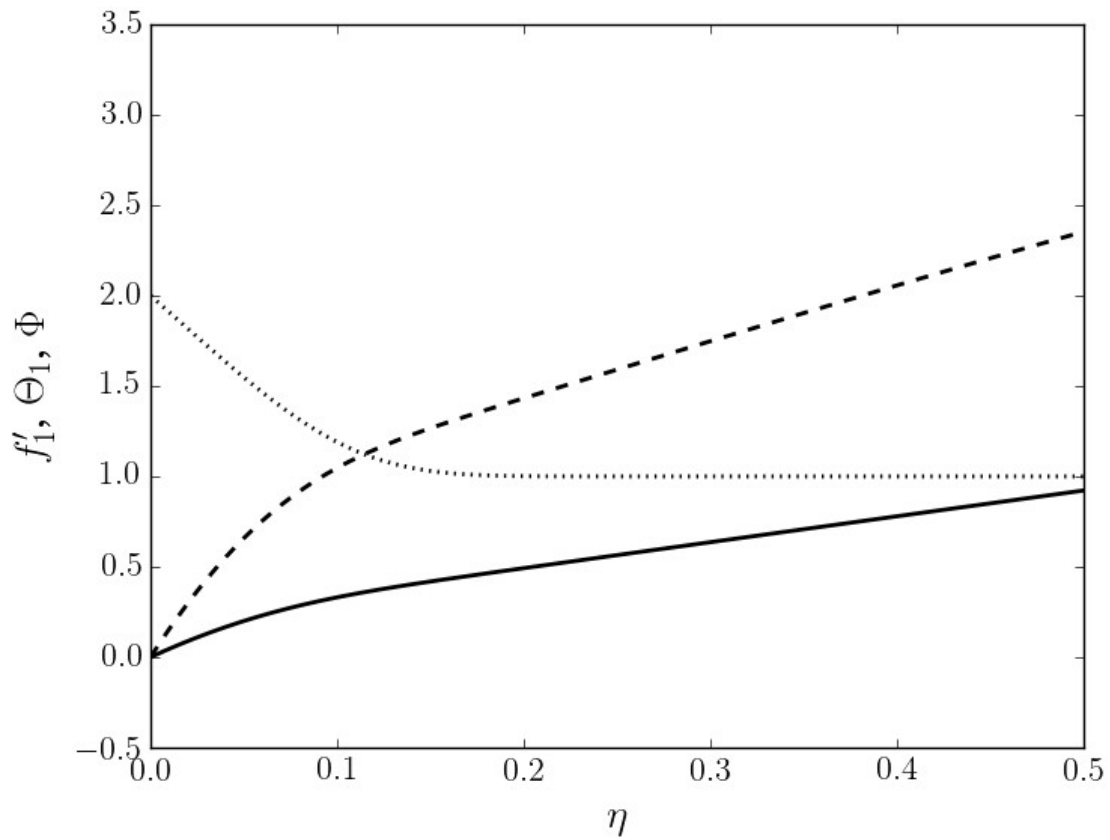


Figure 10b. Wall region, gold-water nanofluent (MD).  $\Phi(0; Sc_f) = 2$   
 $f'_1(\eta)$ : \_\_\_\_\_,  $\theta_1(\eta; Pr_f)$ : - - - - - ,  $\Phi(\eta; Sc_f)$ : .....  
 $Pr_f = 7$ ,  $Sc_f = 2 \times 10^4$



Cintia Juliana Barbosa de Castilho is a Ph.D. student in the Laboratory for Environmental and Health Nanoscience, School of Engineering, Brown University. She received her bachelor's degree of Chemical Engineering at Federal University of Pernambuco, Brazil in 2015. She is currently working on macromolecular imprinting of **two-dimensional** nanomaterials.



Mark Fuller is a Ph. D. candidate under Prof. C. Franklin Goldsmith in Chemical and Biochemical Engineering at Brown University. He received a Master's degree in Chemical Engineering from Brown in 2014 and a Master's in Mechanical Engineering from Cornell University in 2011. His Bachelor's degree in Mechanical Engineering was also completed at Brown in 2009. **His present** work includes design, construction, and operation of a diaphragmless shock tube for investigations of gas-phase chemical kinetics and reaction mechanisms. Other research interests include topics in energy conversion and storage including combustion, batteries, and fuel cells.



Aakash Sane is currently a master's student in Fluids and Thermal Sciences at Brown University. Prior to joining Brown University, he was working as an engineer in the Indian Space Research Organization. He completed his undergraduate degree in Aerospace Engineering from the Indian Institute of Space Science and Technology in 2012. His research interests are in fluid mechanics particularly capillary effects, interfacial phenomenon, and nanofluid flows.



Joseph T. C. Liu is Professor of Engineering in the School of Engineering at Brown University. He received his BSE in Aeronautical Engineering and in Mathematics and MSE from the University of Michigan, and his PhD from the California Institute of Technology where his thesis advisor was the late Professor

Frank E. Marble. He worked in a variety of subjects, including nonlinear instabilities of streamwise vortices with applications to heat transfer enhancement. Of late, he became interested in nanofluid flow and heat transfer enhancement.